

# Model development to calculate explosion and combustion limits in gasification reactors

Master's thesis in Engineering Mathematics and Computational Science

VEENA KANNAN

DEPARTMENT OF MECHANICS AND MARITIME SCIENCES



MASTER'S THESIS IN ENGINEERING MATHEMATICS AND COMPUTATIONAL SCIENCE

Model development to calculate explosion and combustion limits in  
gasification reactors

VEENA KANNAN

Department of Mechanics and Maritime Sciences  
Division of Energy Conversion and Propulsion Systems  
CHALMERS UNIVERSITY OF TECHNOLOGY

Göteborg, Sweden 2023

Model development to calculate explosion and combustion limits in gasification reactors  
VEENA KANNAN

© VEENA KANNAN, 2023

Department of Mechanics and Maritime Sciences  
Division of Energy Conversion and Propulsion Systems  
Chalmers University of Technology  
SE-412 96 Göteborg  
Sweden  
Telephone: +46 (0)31-772 1000

Cover:  
Illustration of a chemical explosive mixture forming within a gasification reactor

Chalmers Reproservice  
Göteborg, Sweden 2023

Model development to calculate explosion and combustion limits in gasification reactors  
Master's thesis in Engineering Mathematics and Computational Science  
VEENA KANNAN  
Department of Mechanics and Maritime Sciences  
Division of Energy Conversion and Propulsion Systems  
Chalmers University of Technology

## ABSTRACT

The combined heat and power (CHP) plants used for district heating and electricity supply has seasonal and daily variations in demand. The thermal capacity of the boilers is thus under-utilized which is tapped into by Bioshare AB. They develop fluidized bed reactors, a well-established technology in Sweden's energy sector. These reactors can be integrated with the boiler plant to transform them into polygeneration units. Liquid and gaseous biofuels, biochemicals and biochar derived from biomass during the pyrolysis reaction within the reactor, extends the product portfolio of the CHP plants making it a financially attractive and a sustainable option. Thus, Bioshare aims to transform the existing co-generating CHP plants into polygeneration units.

While integrating the reactor with the boiler, the fluidized bed is split and exchanged between the two units. The boiler has an oxygen rich environment, and the reactor is oxygen deficient. Both environments are separated by particulate fluidized bed material that is exchanged. This poses a safety risk as oxygen could leak along with the transfer of the bed material from the boiler into the reactor. During the turn down operation of the reactor, the remaining products from the pyrolysis reaction on reacting with oxygen can cause a spontaneous explosion. This thesis work studied the ignition limits of this explosion. Using Cantera software, a numerical model was built to study the ignition delay time under varying conditions. The model presents a 0-dimensional transient problem. By using a surrogate pyrolysis oil composition, the input reaction mechanism file was given from Bioshare. The results from the analysis align with the expected behavior of ignition delay as the pressure, temperature and equivalence ratio varies.

Keywords: combined heat and power plants, fluidized Bed, Cantera, ignition delay



## PREFACE

This Master thesis project was carried out at the Division of Energy Conversion and Propulsion Systems, Chalmers University of Technology during the spring of 2023 in cooperation with Bioshare AB, Sweden.

## ACKNOWLEDGEMENTS

I would like to thank my supervisors Andrei Lipatnikov, Anna Köhler and Gabriel Gustafsson for sharing their expertise and providing valuable guidance during this thesis work. I am grateful for their technical insights and mentorship. I am also thankful to Bioshare AB for providing me with this opportunity. I thank the Division of Energy Conversion and Propulsion Systems at Chalmers University of Technology for the supportive environment during the entire duration of my thesis work. I would also like to thank Pratheeba Chanda Nagarajan for her valuable feedback and support. I also express my gratitude to the examiner, Jonas Sjöblom, Head of Unit, Mechanics and Maritime Sciences, for his guidance and interest in the project. It has been a great learning experience for me. Finally, I thank my family and friends for their constant support and motivation that has helped me in my work.



# List of Figures

1.1	Total energy supply and the contribution of different energy sources in Sweden [4] . . . . .	1
1.2	LULUCF sector emissions and removal of carbon dioxide in EU [13] . . . . .	3
1.3	Recirculation of exhaust steam from steam turbine for heat generation in CHP plants . . . . .	4
1.4	Fluidized Bed reactor showing the bed material in a dynamic fluidized state expanding across the volume of the reactor [17] . . . . .	5
1.5	Converting a cogeneration CHP plant to a polygeneration plant by integrating a fluidized bed endothermic reactor to the fluidized bed boiler plant . . . . .	6
1.6	Sources leading to the formation of the explosive mixture within the endothermic reactor . . . . .	7
2.1	Composition representing a simplified mechanism with reactants used in the numerical model . . . . .	10
2.2	Temperature vs time graph showing ignition delay measured based on different criteria (figure not to scale) . . . . .	13
2.3	Energy diagram for a chemical reaction (figure not to scale) . . . . .	14
2.4	Arrhenius plot [23] . . . . .	14
2.5	Log of ignition delay time vs 1/Temperature . . . . .	15
3.1	Gas mixture composition data of reactants from Bioshare that forms the explosive mixture within the endothermic reactor . . . . .	18
4.1	Temperature vs time plot for given gas mixture with 0.5 equivalence ratio . . . . .	21
4.2	Rate of change of mole fraction of reactant and product species when equivalence ratio = 0.5 . . . . .	22
4.3	Rate of change of mole fraction of the radical species OH when equivalence ratio = 0.5 . . . . .	22
4.4	Temperature vs time plot for given gas mixture with 1.0 equivalence ratio . . . . .	23
4.5	Rate of change of mole fraction of reactant and product species when equivalence ratio = 1.0 . . . . .	23
4.6	Rate of change of mole fraction of the radical species OH when equivalence ratio = 1.0 . . . . .	24
4.7	Temperature vs time plot for given gas mixture with 1.5 equivalence ratio . . . . .	24
4.8	Rate of change of mole fraction of reactant and product species when equivalence ratio = 1.5 . . . . .	25
4.9	Rate of change of mole fraction of the radical species OH when equivalence ratio = 1.5 . . . . .	25
4.10	Ignition delay time behaviour . . . . .	26
4.11	Logarithm of ignition delay time vs temperature inverse . . . . .	27

# Nomenclature

$\dot{A}_{in}$	Flow rate of species A entering reactor
$\dot{A}_{out}$	Flow rate of species A leaving reactor
$\dot{A}_{converted}$	Conversion rate of species A
$\dot{Q}_{in}$	Rate of heat added in reactor
$\dot{Q}_{out}$	Rate of heat removed from reactor
$\dot{Q}_{gen/abs}$	Rate of heat generated and/or absorbed in the chemical reaction
$m_{fuel}$	Mass of fuel
$m_{ox}$	Mass of oxidizer
$n_{fuel}$	Number of moles of fuel
$n_{ox}$	Number of moles of oxidizer
$\dot{m}$	Rate of change of mass
$\dot{m}_{wall}$	Rate of change of mass at the reactor wall
$\phi$	Equivalence ratio
$\tau$	Ignition delay time
$A', B'$	Constants
$A$	Arrhenius factor or the pre-exponential factor
$A_w$	Wall surface area
$c_v$	Heat capacity at constant volume
$E_a$	Activation energy for the chemical reaction
$f_w$	Facing of the reactor wall
$k$	Reaction rate constant
$R$	Universal gas constant
$T$	Temperature
$T_{ref}$	Reference temperature for ignition delay model
$U$	Internal energy
$u$	Specific internal energy
$V$	Volume of reactor
$v_w$	Wall velocity
$Y_k$	Mass fraction of species k

## LIST OF ACRONYMS

<b>CHP</b>	Combined heat and power
<b>CRECK</b>	Chemical Reaction Engineering and Chemical Kinetics group
<b>DLUC</b>	Direct Land use change
<b>EU</b>	European Union
<b>FBC</b>	Fluidised Bed Combustion
<b>GHG</b>	Greenhouse gas
<b>IDLUC</b>	Indirect Land use change
<b>LULUCF</b>	Land use, land use change, and forestry
<b>RHS</b>	Right Hand Side
<b>UN</b>	United Nations



# CONTENTS

<b>Abstract</b>	<b>i</b>
<b>Preface</b>	<b>iii</b>
<b>Acknowledgements</b>	<b>iii</b>
<b>List of Acronyms</b>	<b>vii</b>
<b>Contents</b>	<b>ix</b>
<b>1 Introduction</b>	<b>1</b>
1.1 Motivation . . . . .	1
1.1.1 Land use, land use change, and forestry (LULUCF) activities . . . . .	2
1.2 Background . . . . .	3
1.2.1 Combined heat and power plant . . . . .	3
1.2.2 Fluidized Bed . . . . .	4
1.3 Task Description . . . . .	5
1.4 Objectives . . . . .	7
1.5 Limitations . . . . .	8
<b>2 Theory</b>	<b>9</b>
2.1 Reaction mechanism . . . . .	9
2.2 Chain Reactions . . . . .	11
2.3 Chemical kinetics . . . . .	11
2.4 Ignition delay . . . . .	12
2.5 Arrhenius Law . . . . .	13
2.6 Reactor model . . . . .	15
<b>3 Numerical study</b>	<b>17</b>
3.1 Input parameters . . . . .	17
3.2 Method . . . . .	19
<b>4 Results and Discussion</b>	<b>21</b>
4.1 For Equivalence ratio = 0.5 . . . . .	21
4.2 For Equivalence ratio = 1.0 . . . . .	23
4.3 For Equivalence ratio = 1.5 . . . . .	24
4.4 Ignition delay comparison study . . . . .	26
4.5 Temperature dependency . . . . .	27
<b>5 Conclusion</b>	<b>28</b>
5.1 Future work . . . . .	28
<b>Bibliography</b>	<b>29</b>
<b>References</b>	<b>29</b>
<b>A Appendix</b>	<b>31</b>
<b>B Appendix</b>	<b>37</b>
<b>C Appendix</b>	<b>40</b>



# 1 Introduction

## 1.1 Motivation

Climate change denotes the long-term change in weather conditions. Such changes can be caused by the occurrence of natural events. But in recent years, climate change has been rapid, faster than it has increased at any time in at least the last two thousand years, making it a crucial global issue to discuss [1]. The main driver of such climate shifts is the burning of fossil fuels such as coal, oil, and natural gas. The burning of these nonrenewable fuels generates greenhouse gases like carbon dioxide, methane, nitrous oxide, etc. Greenhouse gas emissions increase the temperature of the earth by trapping heat. The rapid increase in temperature due to various human activities, including deforestation, agriculture, industrial processes, changes in land use, exhaust and non-exhaust emissions from the transport sector, etc., is a huge cause for concern.

The rise in global temperature causes more frequent extreme weather events, such as droughts, hurricanes, and floods. Damages include rapid melting of glaciers in the poles, disturbance of the ecosystem, and rise in sea level, which consequently leads to coastal flooding. Climate change also has a negative impact on soil quality, in turn affecting agriculture and food supply [2]. Unless greenhouse gas emissions fall dramatically, the global temperature increase could reach up to 2.9 ° C in the present century, which could have drastic consequences [3]. Global frameworks and policies such as the Sustainable Development Goals, the UN Framework Convention on Climate Change, and the Paris Agreement are structured to address and combat the climate crisis [1]. One way of reducing GHG emissions is through decarbonization, by increasing the usage of renewable sources of energy.

According to [4], renewables make up 41% of Sweden’s total energy supply as of 2019, as shown in the figure 1.2. The high usage of sustainable sources of energy contributes to Sweden’s low carbon emissions. Hydropower (from moving water) and bioenergy (from biomass) are the two main renewable energy sources in Sweden: hydropower is used mainly for electricity production and bioenergy for heating purposes [5]. Around 60% of Sweden’s renewable energy is bioenergy from biomass. With the availability of a high forest area per capita in the country, the majority (almost 80%) of this bioenergy comes specifically from solid biomass. Bioenergy can be used for power generation, heating for industrial and residential buildings, and also as a transportation fuel [6]. The most common application of bioenergy is in the heating sector. Almost 70% of the fuels used for heating in Sweden come from bioenergy [4].

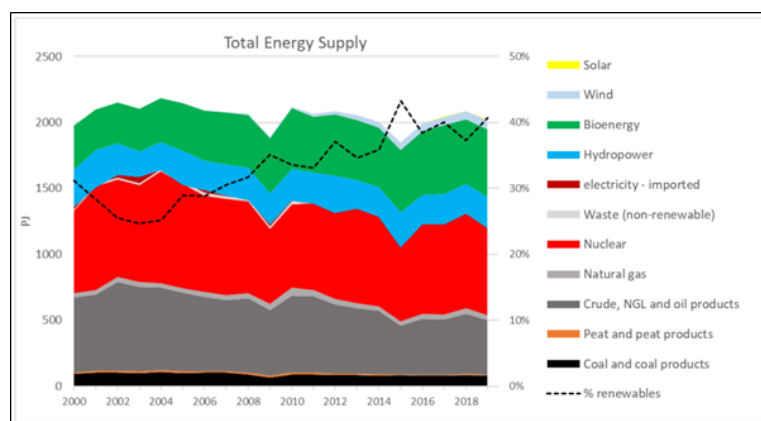


Figure 1.1: Total energy supply and the contribution of different energy sources in Sweden [4]

Observing the trend of renewables % from figure 1.2, we can see that there has been a steady growth of renewable energy sources in Sweden over the past two decades. With the pressing need to combat climate change, we can conclude that this trend will likely continue in the future. This growing presence of biomass increases its scope and potential in Sweden’s energy market. This thesis study is based on one such biomass-derived industrial process.

Bioenergy is derived from biomass, i.e, organic material from plants and animals. When biomass is burned as a fuel source, the carbon released during combustion is neutralized to a certain extent, if not completely, by the carbon dioxide absorbed by plants during photosynthesis in the early stages of the life-cycle of biomass. Thus, bioenergy is considered a cleaner or potential near zero-emission alternative to fossil fuels [7]. Biomass can be burned directly for heat or converted into high-value end products such as liquid and gaseous biofuels, biochar, bioplastics, biofibres, biobased adhesives, etc. through various energy conversion processes.

Biomass energy sources include the following [8]:

- Wood and wood residues (round wood, sawdust and wood scraps)
- Agricultural crops including herbaceous and woody energy crops; agricultural waste residues (straw, leaves, husk, stem, etc.)
- Municipal solid waste—paper, cotton, and wool products from households, commercial/retail shops, etc.
- Animal manure and human sewage to produce biogas / renewable natural gas

However, certain methods of bioenergy production can also have negative environmental impacts. For e.g., the maintenance of large monocultural biofuel farms is not sustainable. The amount of land needed to grow crops for biomass production to satisfy fuel demands is high. An unintended consequence of increasing biomass production is the type of land used for biomass cultivation, further discussed in the following subsection. It might displace agricultural production activities, lead to deforestation, degradation of biodiversity, cause possible food insecurities and have other socioeconomic effects [9]. A careful and detailed evaluation of all the direct and indirect environmental impacts of biofuel production in its entire life cycle will improve our understanding and help plan bioenergy development in a more sustainable way.

### 1.1.1 Land use, land use change, and forestry (LULUCF) activities

The land use sector plays a critical role in combating climate change. Agricultural and forest lands covers more than three-quarters of EU's territory, providing a huge scope to remove carbon dioxide from the atmosphere and reduce GHG emissions. Land use is the management of cropland, grassland, wetlands, forests, settlements and includes land use change such as afforestation, deforestation, or change of agricultural production activities [10].

Lands can be a carbon sink - where more carbon is absorbed from the atmosphere than it emits, through plants cultivated in the area. It can also act as a carbon source - releasing more carbon dioxide into the atmosphere. The usage and management of the land use sector contributes in climate mitigation. The observation and measurement of land use change can be classified as Direct Land use change (DLUC) and Indirect Land use change (IDLUC). The former change is measured when a new activity occurs on a land while the latter is when there an unintentional consequence of land use decisions from elsewhere [11]. Indirect land use change is harder to measure but can give a clearer overall picture, for e.g., deforestation of forest areas or ploughings of grasslands for land use change into croplands can lead to a significant increase of greenhouse gas emissions due to land conversion.

The current EU land use sector absorbs more greenhouse gases than it releases into the atmosphere, making it a carbon sink. One of the EU targets in the European Climate Law is to have net zero green house gas emissions, in other words, to be climate neutral by the year 2050. This does not imply that green house gas emissions would be completely absent, but rather 'unavoidable' emissions will need to be neutralized by carbon removal processes from the atmosphere. However, the Commission noted that the EU is currently not on track to reach its goal by 2050 [12]. This would require scaling up carbon capture solutions, including industrial processes and using natural ecosystems. Unfortunately, carbon removal naturally through the EU land use sector has been seen to be decreasing in recent years [13]. To combat this trend, the Commission has proposed frameworks that incentivize carbon removal activities [14]. Net carbon dioxide emissions from the LULUCF sector and their projected trends from the European Environment Agency, 2022, are depicted in the figure below.

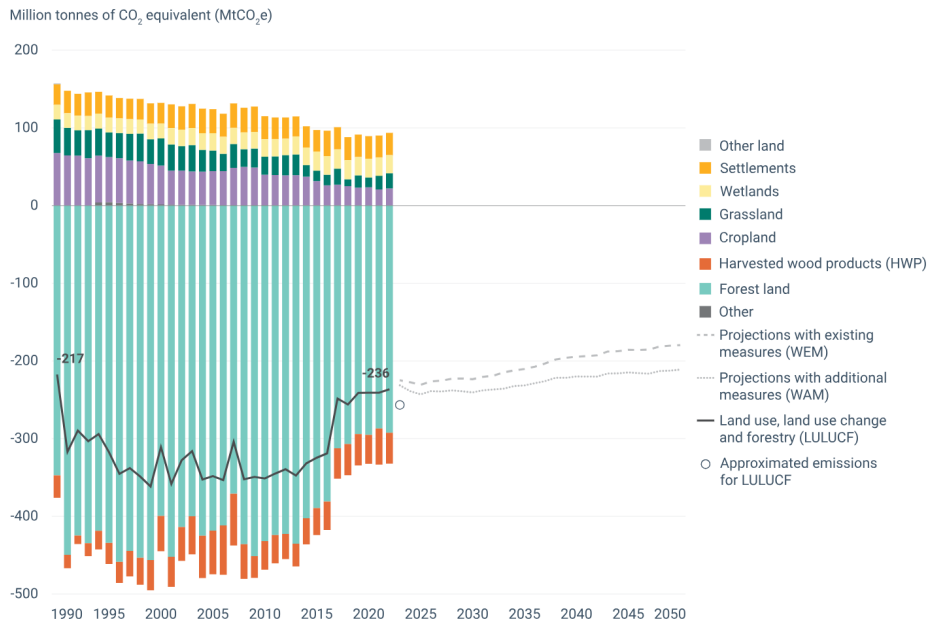


Figure 1.2: *LULUCF sector emissions and removal of carbon dioxide in EU [13]*

## 1.2 Background

The master thesis work is offered by Bioshare AB, whose vision is to transform large-scale combustion plants into biorefineries. Combined heat and power (CHP) plants from biomass and waste-fired boilers used for district heating networks and electricity supply for energy-intensive industry processes have seasonal and daily variations in demand. Due to fluctuations in demand, the installed thermal capacity of the boilers is under-utilized. Taking advantage of this potential, Bioshare aims to transform existing cogenerating CHP plants into polygeneration units through their original concept of chemical reactors for co-pyrolysis or co-gasification. Reactors are integrated into combustion plants internally or externally. The integration of the reactors is tailor-made for each case depending on the boiler plants involved and the needs of the end user. The thermochemical conversion process of gasification/pyrolysis within the reactor also varies with each case.

### 1.2.1 Combined heat and power plant

CHP plants use cogeneration technology that simultaneously produces electricity and heat using a variety of technologies and fuels. Separate power and heat generation results in nearly two-thirds of the energy being wasted, discharged into the atmosphere as heat during the generation, transmission, and distribution stages [15]. By capturing and utilizing heat that would otherwise be lost, CHP plants have a higher efficiency of more than 80%, compared to 50% in conventional technologies [15]. Due to this increased net efficiency, CHP systems emit less carbon emissions than separate heat and grid power generation.

As shown in Figure 1.3, the thermal energy from the combustion of fuel within the boiler plant converts water to steam. The steam is then passed through a steam turbine to generate electricity. The thermal energy from the used steam leaving the steam turbine is then recirculated for heat generation. This is the basic working idea of a CHP plant used for district heating and electricity supply.

Biomass based CHP is a well-established industry in Sweden. By converting cogeneration CHP plants to polygeneration units, as shown in Figure 1.5, Bioshare increases the utilization of these plants by increasing their product portfolio to include renewable products like energy gas, biofuels, pyrolysis oil and biochar, in addition to heat and power produced by the boiler plant. CHP plants use fluidized bed technology, a technical process that enables high surface area contact, excellent heat and mass transfer, and an increased reaction rate.

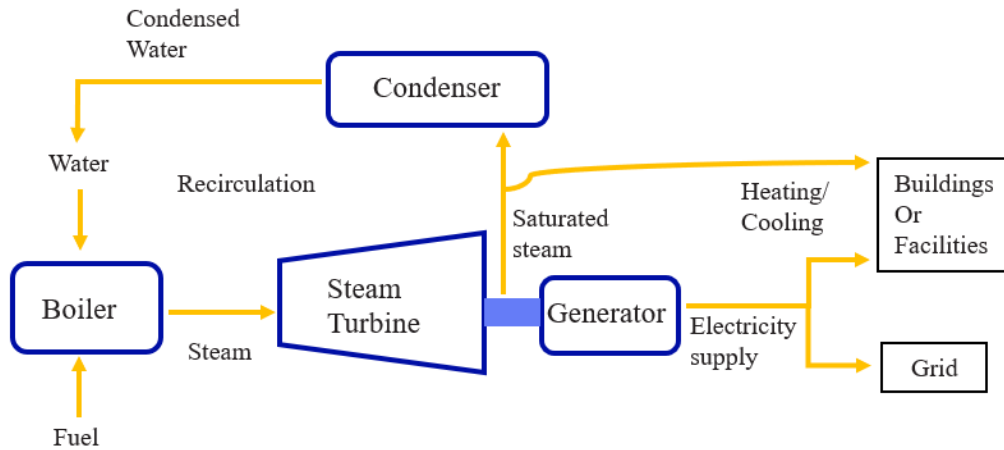


Figure 1.3: *Recirculation of exhaust steam from steam turbine for heat generation in CHP plants*

### 1.2.2 Fluidized Bed

Fluidized bed technology is used in both the boiler during combustion and in the reactor during the pyrolysis/-gasification reaction. The bed rests on an air distributor grid. The air used as the fluidization gas for the boiler is also used in the combustion process to burn the fuel. The fluid/air is allowed to flow upward through the solid particulate bed material at high velocities that suspend the solid bed and force it to behave like a fluid. At low velocities of the air, the bed remains in its place. Once it crosses a certain minimum fluidization velocity threshold, the bed material circulates across the reactor. The reactor is now a fluidized bed, as shown in Figure 1.4. Depending on the gas velocity value, the mode of fluidization of the bed can be classified as a stationary (bubbling) fluidising bed or a moving (circulating) fluidising bed. The fluidized bed is made up mainly of an inert material that has a large thermal capacity. In a circulating fluidized bed chamber, this property of the inert material evens out the temperature variations and forms a thermally stable environment. This is one of the main features of a fluidized bed, it helps maintain a uniform temperature across the entire volume of the boiler/reactor. The bed transfers the heat from the respective chemical reactions that occur within the boiler/reactor. Fluidized beds are used in the industry since they offer advantages like uniform particle mixing, maintaining uniform temperature gradients, and the possibility to run the reactor continuously [16].

Combustion of the biomass in the boiler produces heat, while thermochemical conversion processes like pyrolysis and gasification produce convenient energy carriers like biochar, liquid and gaseous biofuels. Biomass can be converted to energy through combustion to produce heat. Biomass can also be converted to solid, gaseous, and liquid fuels through thermochemical conversion processes like pyrolysis and gasification. The principal product from the combustion reaction is heat that is used to generate steam to produce electricity. However, in gasification and pyrolysis reactions, the combustible solid, gaseous and liquid products have calorific/heating values (the amount of heat released on the combustion of a specific amount of fuel). Combustion is an exothermic process, while gasification and pyrolysis are endothermic reactions that pack energy into chemical bonds. Pyrolysis and gasification differ in the temperatures and amount of oxygen present during the thermal decomposition processes. Gasification occurs at temperatures close to 1000 °C with a minimum amount of oxidizer present, while pyrolysis occurs in the absence of an oxidizer at temperatures comparatively lower around 300 °C to 600 °C.

The fluidized bed can have a fixed or moving bed made of inert granular material, classified as bubbling or circulating fluidized bed, respectively. The solid particulate bed is initially at rest. Streams of gas, termed fluidization gas, flow through the bed material. The fluidization gases upon crossing a particular threshold

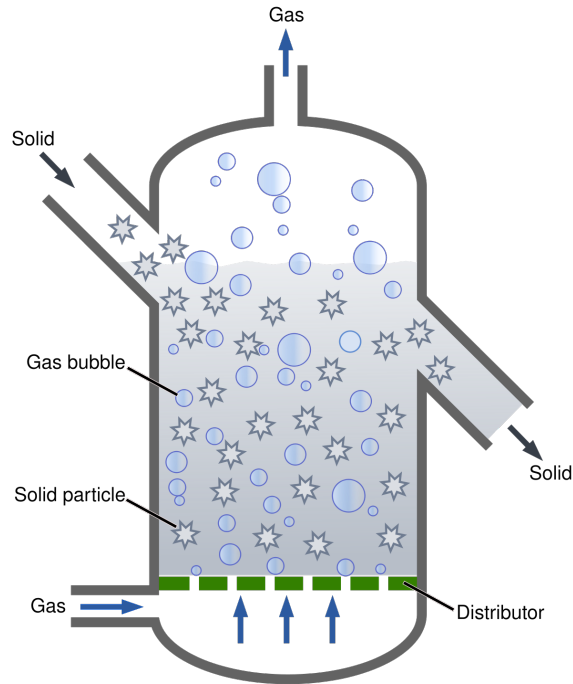


Figure 1.4: *Fluidized Bed reactor showing the bed material in a dynamic fluidized state expanding across the volume of the reactor [17]*

velocity circulate the bed material, making it behave like a fluid. The bed material has a high heat capacity and helps spreading the heat from the combustion reaction uniformly across the volume of the plant. The following subsection describes the specific setup problem of the integrated reactor with the FB boiler plant at Bioshare AB.

### 1.3 Task Description

Bioshare AB develops the original concepts of an endothermic chemical reactor in which a pyrolysis / gasification reaction occurs that is integrated with the boiler plant, illustrated in figure 1.5. The fluidized bed is used in both the boiler and the endothermic reactor units. For the fluidized bed in the boiler plant, air is used as the fluidization gas. The oxygen from the air is utilised in the combustion reaction. The flue gas byproduct from the combustion reaction is the fluidization gas in the chemical reactor. After the combustion reaction within the boiler, the hot bed material is transferred to the reactor. Along with this bed material transfer, a part of the thermal energy from the exothermic reaction in the boiler is transferred to the endothermic reactor and used for the pyrolysis/gasification chemical reaction. The bed material is then recirculated back to the boiler along with the carbon-rich biochar product from the pyrolysis reaction.

During the endothermic reaction, a minimum amount of oxygen is maintained within the chemical reactor. Since the oxygen rich boiler environment and the oxygen deficient chemical reactor environment is separated only by the particulate bed material with air being exchanged along with it, oxygen might escape from the boiler into the reactor. In such scenarios, an increase in the concentration of oxygen in the chemical reactor might react with the left-over products from the pyrolysis reaction and cause a chemical explosion. This poses a safety risk to the reactor during its turn down operation. The focus of this thesis is on further understanding and investigation of the parameters of this explosion for safety reasons.

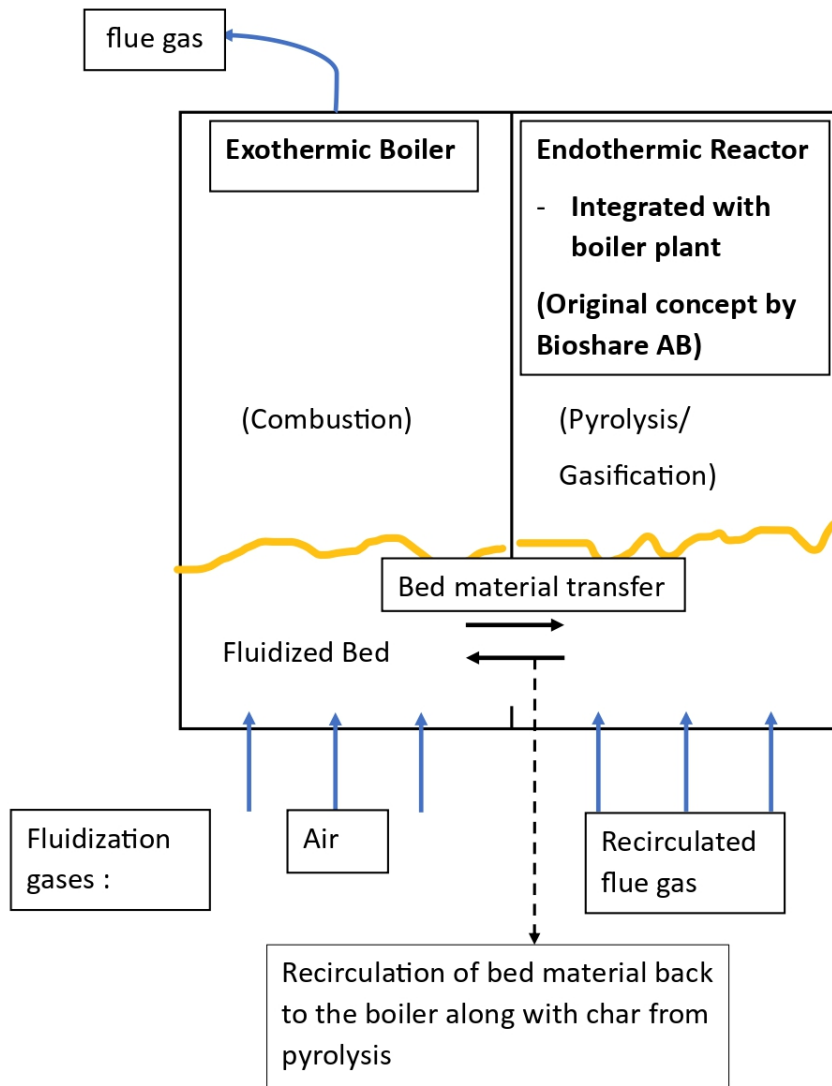


Figure 1.5: *Converting a cogeneration CHP plant to a polygeneration plant by integrating a fluidized bed endothermic reactor to the fluidized bed boiler plant*

The thesis task is to study the conditions that lead to the chemical explosion within the reactor and its impact. There are chances of air and flue gas escaping through the bed material into the reactor, leading to the explosion. The maximum chance of an explosion occurring is during the turn down operation of the reactor, when escaped air and flue gas chemically react with the pyrolysis reaction products. Flue gas is the combustion exhaust gas from the boiler, whereas the pyrolysis reaction end products are combustible fuels that possess a calorific value. This is shown above in figure 1.6 as the constituents of the combustible mixture formed.

The pyrolysis products can be classified into two groups as condensable/volatile that are gaseous within the high-temperature reactor environment and liquid under room temperature conditions, and permanent gas products that remain gaseous at room temperature. The exact gas mixture composition of the condensables from the pyrolysis reaction is complex and unknown. A reduced reaction mechanism is used in the numerical model as an estimate to the actual volatiles formed.

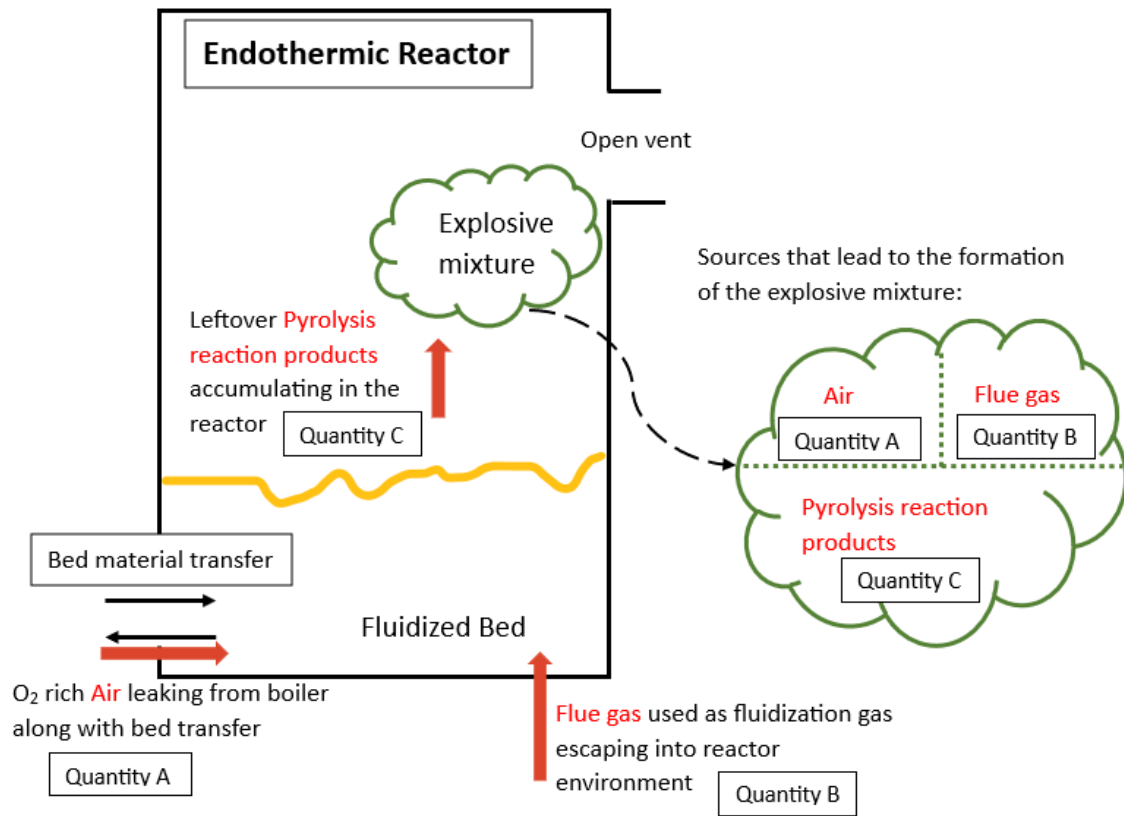


Figure 1.6: Sources leading to the formation of the explosive mixture within the endothermic reactor

During the turn down operation of the reactor, possible sources causing the formation of the explosive mixture:

- Air escaping into the reactor from the boiler plant during bed material transfer
- Flue gas leaking into the reactor environment when passed through the granular fluid bed
- Accumulation of the permanent gas products and condensables from the pyrolysis reaction in the endothermic reactor which includes energy gas and pyrolysis oil

## 1.4 Objectives

The purpose of this thesis is to study the conditions that lead to the explosion within the reactor and the resulting maximum pressure calculation from the vented gas explosion. Combustion reactions, such as those in the boiler, are controlled chemical reactions when the fuel reacts in the presence of oxygen at suitable temperature and pressure conditions to release energy. It usually happens in a monitored environment. On the other hand, explosions are uncontrolled chemical reactions that violently release huge amount of energy rapidly in an extremely short frame of time. Explosive chemical reactions are usually dangerous and unintended and pose a safety hazard. These explosions occur in a fraction of seconds when the conditions suitable for the start of chemical reactions are achieved. The conditions include favorable temperature, pressure, and chemical compositions. The time span or lag of time that it takes to reach these favorable conditions and initiate the chemical reactions is called ignition delay time. In this thesis work, a specific study and prediction of the ignition delay time is performed for the given problem scenario. The purpose of this work is to better understand the conditions of the explosion limits through modeling, detailed in the following paragraph. The

results of this model will aid in better understanding of the safety conditions and design limits of the gasification reactor.

1. Investigate and understand the conditions under which the gas explosion occurs for varying parameters: equivalence ratio, pressure, and temperature. The ignition delay time is mapped for the following conditions:
  - (a) Pressure within the range of approximately 0.6 bar and 1.5 bar, split uniformly at 5 levels, i.e, at values 0.61, 0.84, 1.06, 1.29 and 1.52 bar
  - (b) Temperature at values 650, 750 and 850 °C
  - (c) Equivalence ratio at values 0.5, 1 and 1.5
2. Derive a model and calculate the maximum pressure increase resulting from the vented explosion in the chemical reactor.

## 1.5 Limitations

- The exact mixture of the gas components that form the condensables in the pyrolysis reaction is unknown. A surrogate pyrolysis oil composition with important selected chemical species that is good enough to mimic the behavior of the actual composition was suggested.
- A reduced reaction mechanism file estimating the significant chemical kinetic and combustion properties of the combustible mixture is used.
- The gas mixture is assumed to behave like an ideal gas.
- The problem is modeled as a 0-dimensional transient problem. This assumption ignores the variations of pressure in space.

Pressure fluctuations in space travel at the speed of sound, which varies based on the composition and the temperature of the medium. The higher the temperature and pressure conditions, as in the case of the gasification reactor, the faster the pressure variations travel. The pressure variations travel at a much faster rate than the time scale of the ignition delay phenomena observed. Thus, the assumption of reducing the model to 0-dimensional holds.

- The reactor is assumed to be a closed fixed volume adiabatic system which is not the case in reality.

## 2 Theory

The amount of input data required to model a complex chemical reaction for the explosion in the described endothermic reactor is staggering. It involves the thermodynamic properties of every individual chemical species involved and multiple interacting chemical reactions. An approximate simplified version of the actual mechanism is utilized for practicality. This simplification significantly reduces the amount of data needed for computation. To start with modeling chemical reactions, the input information required can be categorized based on [18]:

- Thermodynamic properties which includes the thermodynamic state of species such as pressure, density, enthalpy, etc. of all the participating chemical species in the explosion.
- Chemical kinetics properties, that is, the information on reaction rates of progress, species production rates, etc., and the detailed elementary reactions that occur during a chemical reaction.
- Transport properties that give information on diffusion, thermal conductivity, viscosity, etc.

These chemical properties are translated as a single input file to build a numerical model in Cantera. Studying the ignition delay process of a chemical explosion reaction requires understanding of many theoretical concepts. This chapter attempts to briefly discuss selected relevant topics. The initial sections of the chapter focus on the input chemical properties used, while the latter half covers topics pertaining to the phenomena and governing laws of ignition delay in a fluidized bed reactor model.

### 2.1 Reaction mechanism

Usually a global/overall chemical reaction with the initial reactants and the final products formed is represented in a theoretical construction of the chemical reaction. The given reactant species do not react with each other all at once to directly form the final products. In reality, there are many other chemical species involved in many intermediate elementary reactions. It is not practical to obtain a complete reaction mechanism file; thus, a simplified reduced mechanism is estimated and used in numerical solutions that include the important species and reactions that might affect the overall reaction rate. Such reduced mechanisms can only be used for a specific range of temperature, pressure, or composition conditions of the mixture.

The condensables from the pyrolysis reaction in the reactor or bio-oils are complex liquid mixtures whose complete chemical composition is unknown. Instead, a surrogate composition of pyrolysis oil is utilized where the most significant classes of chemical species are included to represent the properties of the actual pyrolysis oil. The Pelucchi mechanism model is used to obtain a reliable characterization of the combustion properties of condensables [19].

The interactions of all elementary reactions in a detailed reaction mechanism govern the overall combustion reaction. However, in this complete set of reactions, only a few elementary reactions, called rate-limiting reactions, determine the rate of the overall process [20].

A simplified mechanism with the list of reactant species provided by Bioshare is illustrated in 2.1. The list of product species obtained from the reaction is also shown in the illustration below. This reaction was simulated under the following conditions: pressure = 1 Pa, temperature = 923 K, and equivalence ratio = 1. The model was tested under varying conditions of pressure, temperature, and equivalence ratio. The calculation model used to perform these studies and the specific compositions of reactants used in the numerical model are detailed in the next chapter.

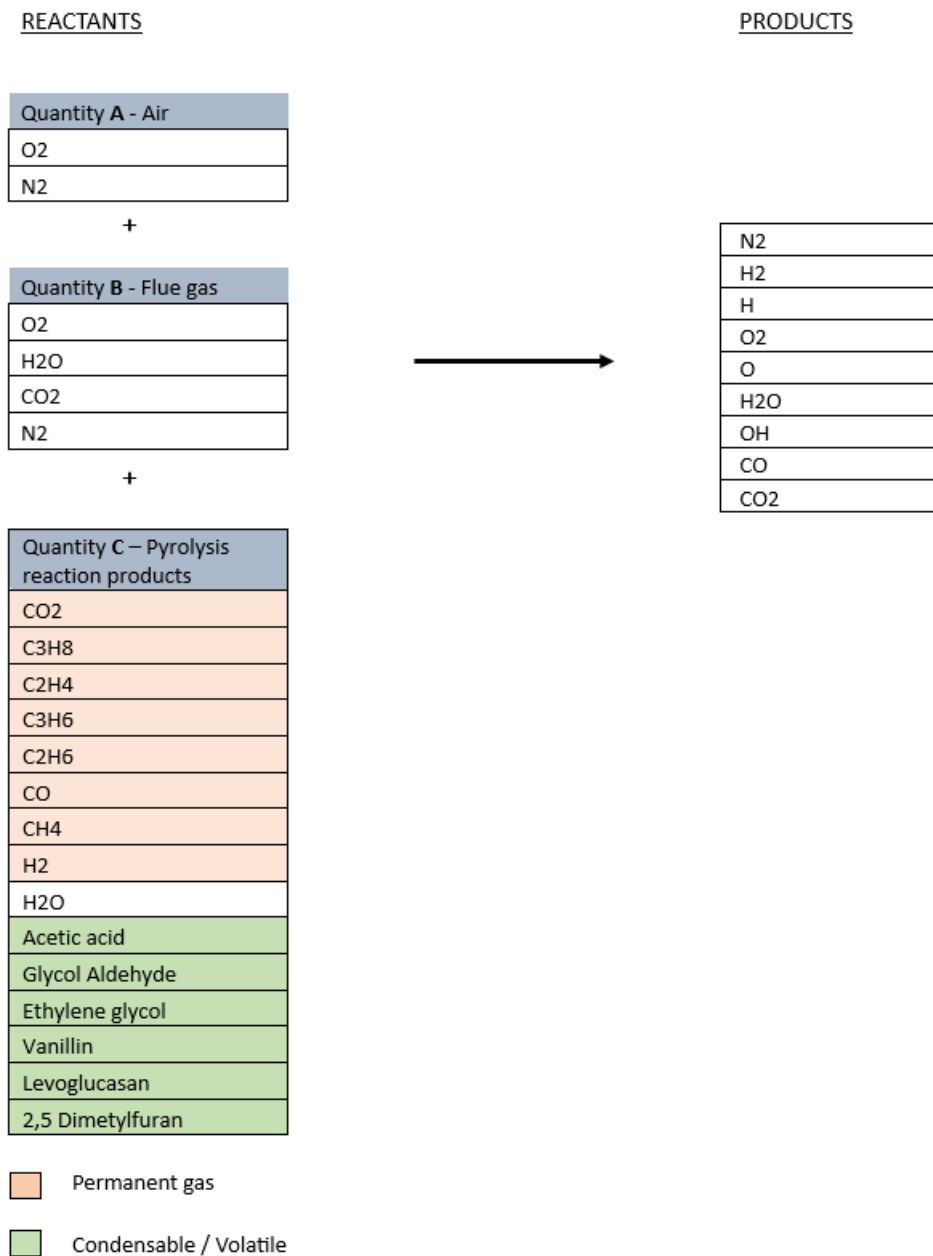
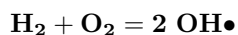


Figure 2.1: Composition representing a simplified mechanism with reactants used in the numerical model

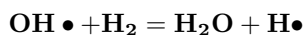
## 2.2 Chain Reactions

There are different types of reactions in a reaction mechanism that forms a chain of reactions. Radicals possess an unpaired electron, making them unstable and highly reactive. In a chemical explosion process, radical chain reactions are crucial. The reaction types are as follows, examples of each reaction type are given with respect to ignition in a hydrogen-oxygen system [20]:

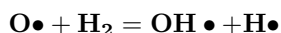
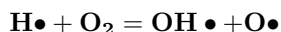
- **Chain initiation** - Reactive species (radicals) are formed from stable species (overall reactants). These reactions often require high temperature to start [21]. For example, in the oxidation of hydrogen, both stable reactants react to form a radical species as shown below.



- **Chain propagation** - Reactive intermediate species react with stable species to form another reactive species. Unlike chain branching reactions, the concentration of free radicals remains the same in these reactions. For example:

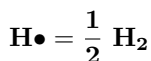


- **Chain branching** - Reactive species reacts with stable species to form more than one reactive species. So, the concentration of reactive species is multiplied by these types of reactions. These reactions are very important for the propagation of flames. For example, in the same hydrogen-oxygen ignition, we see the radical species increasing in concentration, as is shown below.



This exponential increase of radicals happens during the ignition delay time period. The amount of hydrocarbon fuel consumed during this stage and thus the heat released is very little. As a consequence, there is no significant temperature increase [20].

- **Chain termination** - Reactive species are consumed to form stable species(overall products). Also called chain breaking reactions, they usually do not depend on temperatures [21]. Reactive species usually diffuse to the vessel wall where they recombine to form stable species in surface reactions [20]. Example for the same reaction type, where M denotes other intermediate species that are neither the overall products nor reactants :



## 2.3 Chemical kinetics

In thermodynamics, the speed of a chemical reaction is not taken into account and therefore no information is provided on the rate of a chemical reaction. But in the case of practical combustion phenomena such as ignition, explosion, and extinction of flames, the speed at which the chemical reaction occurs is a key driving factor [21]. Chemical kinetics, as opposed to thermodynamics, gives information on the rate of a chemical reaction.

The rate of a reaction depends on the composition of the reaction mixture, the temperature, and the pressure. There are many reaction rate theories to derive a general form of a rate equation. However, they cannot be used to obtain quantitative values for the constants in the rate equation. The constants must be determined experimentally [22].

A general method to find the reaction rate is from the rates of consumption of the reactant species or the rates of formation of the product species. Consider a general case [20]:



Reaction rates based on species concentrations can have many forms, where power law-type expression is common. [22] The reaction rate expressed as the disappearance of species A is expressed as follows [20]:

$$\frac{d[A]}{dt} = -k \cdot [A]^a [B]^b [C]^c \dots \quad (2.1)$$

where [A], [B], [C],... are the concentrations of species A, B, C and so on. a, b, c,... are reaction orders with respect to the species A, B, C,... which is the power dependence of the rate on the concentration of each reactant. k is the rate coefficient of the reaction that can be determined experimentally. The minus signs denote the consumption/disappearance of reactant species A.

The rate equations for simple elementary reactions are straightforward, but complicated for huge reaction mechanisms with many intermediate reactive species [22]. If a complete reaction mechanism is available that contains all possible elementary reactions, rate laws for the individual elementary reactions can be found. The rate of formation or consumption of a chemical species is then given by its summation over the rate expressions of all elementary reactions [20]. However, in practice, complete or detailed mechanisms are rarely available. Instead, a reduced reaction mechanism that uses a smaller set of chemical species, as shown in figure 3.1, that affect the reaction rate, is deduced and used to model combustion reactions.

## 2.4 Ignition delay

Chain branching reactions, as seen above, form the basis for determining the ignition delay time. During the ignition delay time period, the concentration of radicals/reactive species increases at an exponential rate. But the amount of energy released at this stage from the consumption of reactants in the exothermic reaction is too small, and the temperature remains almost constant. Radical accumulation occurs and, once they consume a significant amount of reactants, spontaneous ignition takes place. This releases a large amount of energy, leading to a rapid increase in temperature that causes an explosion [20].

Many different criteria can be used to define ignition delay time, such as measuring fuel consumption, the formation of intermediate radical species such as OH, the increase in pressure in a constant volume vessel, the rate of increase of temperature in an adiabatic system, the time taken to reach a fixed reference temperature value, etc. In this thesis a reference temperature is fixed, denoted as  $T_{ref}$  in figure 2.2, and the time taken to reach that temperature is defined as ignition delay.

A typical temperature vs. time graph to measure ignition delay time is shown in figure 2.2. The graph is divided into 3 sections. The first section shows the initial phase when the conditions are satisfied enough for the reactant species to overcome the activation barrier, which could be an increase in temperature, pressure of the enclosed reactor, an increase in the concentration of specific reactant species through leakage, as discussed previously in Section 1.3 or a combination of the same. Chemical reactions are initiated at this stage. The radicals continue to increase through chain branching reactions during the ignition delay time period  $\tau_1$  in figure 2.2. The second region is where the radical pool buildup becomes large enough to react with a significant amount of stable reactant species and release high energy. This results in a huge and rapid increase in temperature, as seen in stage 2 in figure 2.2. Chain branching reactions are the most important defining set of reactions in a chemical explosion. Chain propagation reactions consume stable species without increasing the concentration of radicals. The third final section seen in the figure is when radicals are consumed to form stable overall product species during chain termination reactions. The temperature change is minimal at this stage of the process.

The  $T_{ref}$  in figure 2.2, used as the reference temperature to define the ignition delay for the purpose of this thesis study, can be defined as the temperature when spontaneous ignition occurs. The autoignition temperature is the minimum temperature at which a fuel/air mixture ignites without an external source. In

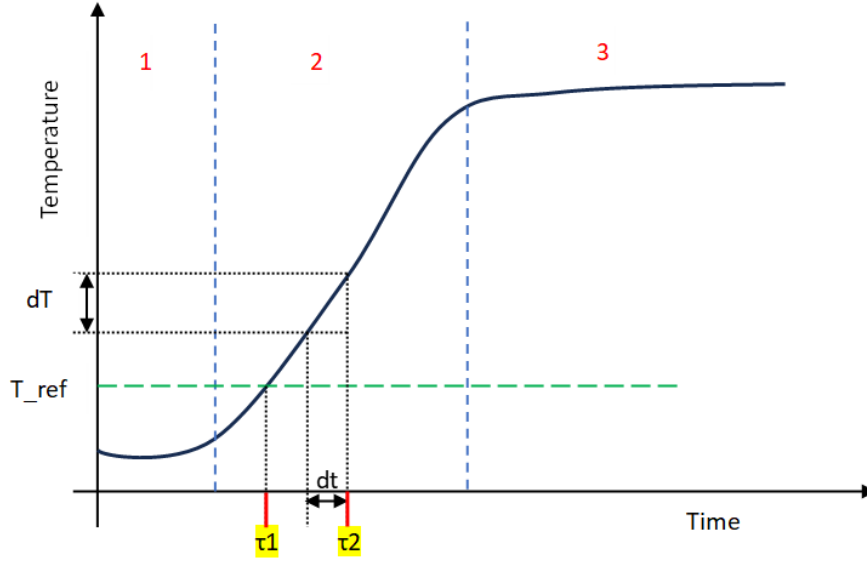


Figure 2.2: *Temperature vs time graph showing ignition delay measured based on different criteria (figure not to scale)*

the built numerical model,  $T_{ref}$  is fixed as 20% above the initial temperature of the mixture. The criteria used to define ignition delay as the time period for the explosive mixture in the gasification reactor to reach the reference temperature,  $T_{ref}$  is denoted as  $\tau_1$  in the figure 2.2. The ignition delay criterion can also be evaluated as the time taken to reach the maximum rate of temperature change, thus measuring the slope  $\frac{dT}{dt}$ , of the graph, and is indicated as  $\tau_2$  in the figure 2.2.

## 2.5 Arrhenius Law

From the previous section, we have seen the expression of the reaction rate formulated in terms of the concentration of the product species and the rate coefficient, equation 2.1. One of the parameters that the rate coefficients strongly depend on is the temperature, which is described by the Arrhenius equation as follows.

$$k = A.exp\left(\frac{-E_a}{RT}\right) \quad (2.2)$$

The Arrhenius equation can be applied to determine the activation energy and the rate of chemical reactions as the temperature changes. The activation energy denotes an energy barrier that the reactants have to overcome in order to form products. It is the minimum energy requirement that is needed for the chemical reaction to occur. The following plot helps us better understand the concept:

From the Arrhenius equation and the figure 2.3, it can be seen that decreasing the activation energy will lower the energy barrier to overcome, making it easier for the chemical reaction to occur. This corresponds to an exponential increase in the reaction rate. Taking the natural logarithm on both sides of the Arrhenius equation 2.2, we get the following.

$$\ln k = \ln A - \left(\frac{E_a}{R}\right)\left(\frac{1}{T}\right) \quad (2.3)$$

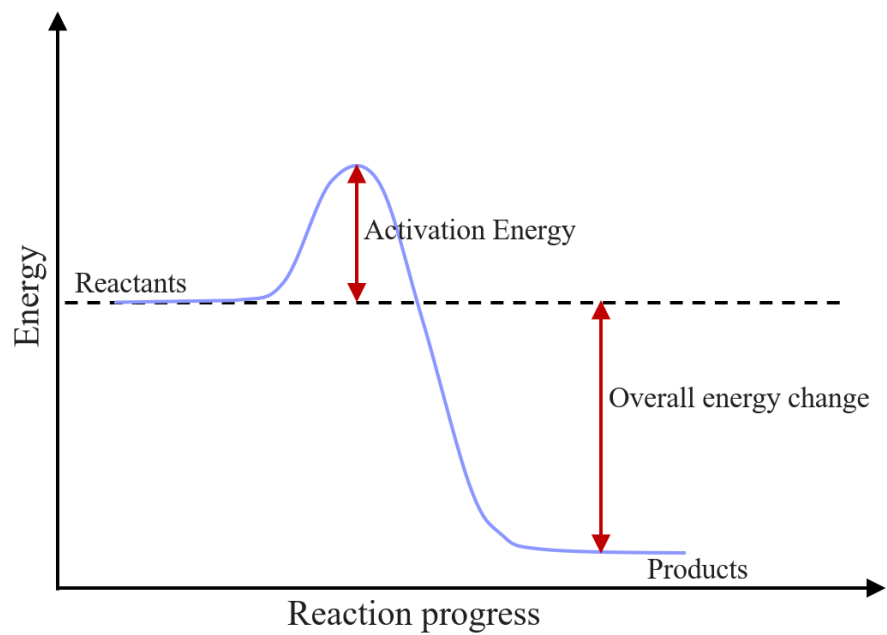


Figure 2.3: *Energy diagram for a chemical reaction (figure not to scale)*

The linearized equation 2.3 above, in the form  $y = mx + b$ , can be plotted to visualize the Arrhenius equation. The plot  $\ln k$  versus  $\frac{1}{T}$  can be used to calculate the activation energy from the slope of the graph, which is  $-\frac{E_a}{R}$ . From the plot, it can be seen that as the temperature reduces, the reaction rate decreases.

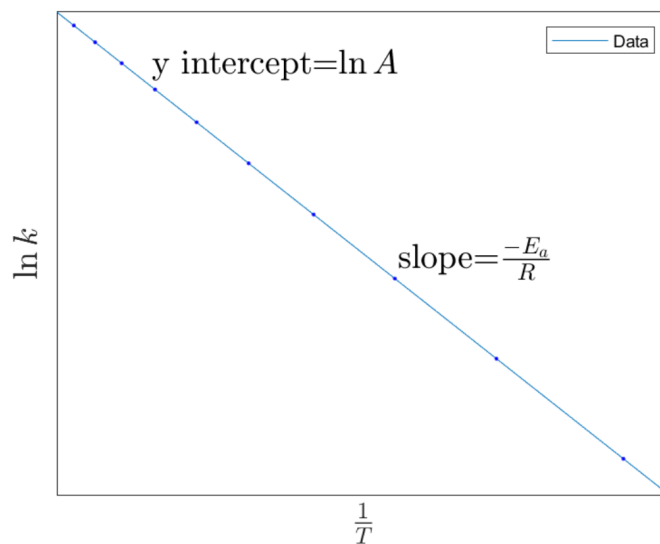


Figure 2.4: *Arrhenius plot [23]*

We had previously seen that the important chain branching reactions happen during the ignition delay time period. The temperature dependence of these underlying reactions can be observed by the strong influence of temperature on the ignition delay time. This is shown in the plot below and reflects the temperature dependence of the elementary reactions occurring during ignition delay time period (Arrhenius law) :

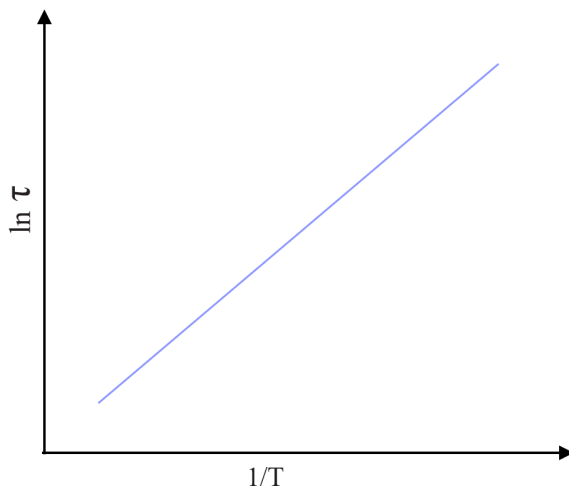


Figure 2.5: *Log of ignition delay time vs 1/Temperature*

Thus, the ignition delay time depends exponentially on the inverse of temperature:

$$\tau = A' \cdot \exp(B'/T) \quad (2.4)$$

where

$A', B'$  are constants,

$T$  is the absolute temperature and

$\tau$  is the ignition delay time.

## 2.6 Reactor model

The chemical reactor is a simple system that has a specific control volume  $V$  within which chemical reactions occur. There are many types of chemical reactors, such as batch reactors, continuous stirred tank reactors, etc. depending on which the governing equations change. The reaction rate equation, equation of state (like the ideal gas equation), continuity, energy, and momentum equations are used to describe a chemical reactor system. The conservation equations for mass, energy, and momentum are discussed qualitatively. The reactor modeled in this thesis is a 0 dimensional closed system and does not have any flow of gas species into or out of the reactor.

Applying the law of conservation of the mass of any species  $A$  to a control volume defined within the reaction [24]:

$$\begin{aligned} & \left( \text{Flow rate of A entering} \right) - \left( \text{Flow rate of A leaving} \right) - \\ & \left( \text{Conversion rate of A} \right) = \left( \text{Rate of change of A} \right) \end{aligned} \quad (2.5)$$

$$\dot{A}_{\text{in}} - \dot{A}_{\text{out}} - \dot{A}_{\text{converted}} = \frac{dA}{dt}$$

This is the species continuity equation giving the mass balance for each individual chemical species in the reaction. They are normally expressed in terms of molar flow [22]. The sum of the continuity equations of all the individual species gives the total mass balance equation for the reactor system.

In the energy equation for a control volume element in a chemical reactor, only the thermal energy resulting from the chemical reaction is considered [24]. Kinetic, potential, and work terms are ignored in comparison to the heat of the reaction. The reactor model applied in this thesis is assumed to be adiabatic, having no heat transfer between the system and the surroundings. The energy equation for a chemical reactor that gives the heat balance of the reactor system is applied over a control volume is as follows.

$$\begin{aligned} & \left( \text{Rate of heat added} \right) - \left( \text{Rate of heat removed} \right) - \\ & \left( \text{Rate of heat generated and/or absorbed in the chemical reaction} \right) = \\ & \left( \text{Rate of heat change} \right) \end{aligned} \quad (2.6)$$

$$\dot{Q}_{\text{in}} - \dot{Q}_{\text{out}} - \dot{Q}_{\text{gen/abs}} = \frac{dQ}{dt}$$

Momentum balance equations provide information on variations in pressure and velocity in space within the reactor. By applying Newton's second law to a fluid particle over a volume element [24], we get:

$$\begin{aligned} & \left( \text{Rate of momentum added} \right) - \left( \text{Rate of momentum removed} \right) - \\ & \left( \text{Sum of forces acting including pressure and shear stress} \right) = \\ & \left( \text{Rate of change of momentum} \right) \end{aligned} \quad (2.7)$$

The equation of state used to describe the system is the equation of the ideal gas:  $PV = nRT$ , where P is the pressure, V is the volume, n denotes the amount of substance, R is the constant of the ideal gas and T is defined as the temperature of the system. An ideal gas reactor is assumed where all gas species in the reactor are assumed to follow the ideal gas law. In an ideal reactor, the momentum balance equation is not used. The specific governing equations used to model the reactor in the simulation study are specified in the next chapter. The reactor system used in the numerical study is 0 dimensional.

## 3 Numerical study

### 3.1 Input parameters

The simulation was carried out using Cantera in Python. The explosive mixture within the reactor is defined as a gas object. As seen previously in figure 1.6, the sources that make up the explosive mixture can be classified into 3 groups: Air, Flue gas and Pyrolysis product species. These three groups, defined as 'quantities' in the Cantera environment, are the input of the chemical composition defined for the gas object. Quantity A is the air leaked from the boiler environment, quantity B is flue gas used as fluidization gas in the chemical reactor and quantity C includes the products from pyrolysis reaction that remain within the chemical reactor during its turn down operation.

The explosive mixture is assumed to be uniformly premixed in the reactor. The reactor is assumed to have a fixed volume and an adiabatic system (where there is no loss of energy to the environment). Thus, the defined Quantities A, B and C are mixed at constant internal energy (denoted as U), since it is an adiabatic system and at constant volume V representing a fixed volume reactor.

The exact chemical composition of the volatiles from the pyrolysis reaction within the reactor is complex and unknown. Some reference chemical species are selected to characterize the properties of the actual bio oil and thus the composition of the surrogate pyrolysis oil is taken as a close estimate. The composition of the surrogate pyrolysis oil given by Bioshare is as shown in the figure 3.1, under condensables within the defined 'Quantity C'. The reaction mechanism input file with detailed kinetics of the pyrolysis oil used in the numerical model was developed by the research group CRECK, Chemical Reaction Engineering and Chemical Kinetics Group. An accurate and reliable characterization of the physical, chemical and combustion properties of pyrolysis oil is important to evaluate its value as an energy producing fuel in real time [19].

The initial temperature for the gas mixture defined above is set for 3 values: 650 °C, 750 °C and 850 °C. The pressure ranges from 0.6 bar to 1 bar, at 5 uniformly split levels. Equivalence ratio values of the mixture are also fixed at values 0.5, 1 and 1.5, which affects the gas composition. The equivalence ratio ( $\phi$ ) of a system is defined as the hydrocarbon-to-oxidizer ratio to the stoichiometric hydrocarbon-to-oxidizer ratio [25]:

$$\phi = \frac{(\text{fuel} - \text{to} - \text{oxidizer ratio})}{(\text{fuel} - \text{to} - \text{oxidizer ratio})_{st}} = \frac{\left(\frac{m_{fuel}}{m_{ox}}\right)}{\left(\frac{m_{fuel}}{m_{ox}}\right)_{st}} = \frac{\left(\frac{n_{fuel}}{n_{ox}}\right)}{\left(\frac{n_{fuel}}{n_{ox}}\right)_{st}} \quad (3.1)$$

where  $m$  is the mass,  $n$  is number of moles and suffix  $st$  stands for stoichiometric conditions.

Quantity A - air is defined as the oxidizer, and Quantities B and C - flue gas and pyrolysis product species, together are taken as the fuel. In a stoichiometric reaction, the theoretical amount of air/oxidizer present is the exact amount required to completely react with the fuel present to form the products. When  $\phi = 1$ , the reaction is stoichiometric; when  $\phi < 1$  the mixture is called a lean mixture, where the fuel present is less than that required for a stoichiometric reaction; and when  $\phi > 1$  the mixture is called a rich mixture, where the fuel is present in excess of that required for a stoichiometric reaction. The adiabatic flame temperature reached is maximum when the mixture composition is stoichiometric. The adiabatic flame temperature is the maximum temperature of the combustible gas mixture that can be reached during the combustion reaction when no heat is lost to the surroundings under adiabatic conditions [26].

Temperature, pressure and equivalence ratio are the three main input parameters that were specified at the previously mentioned values to carry out simulations to study the ignition phenomena. The results of this numerical model are presented and discussed in the next chapter.

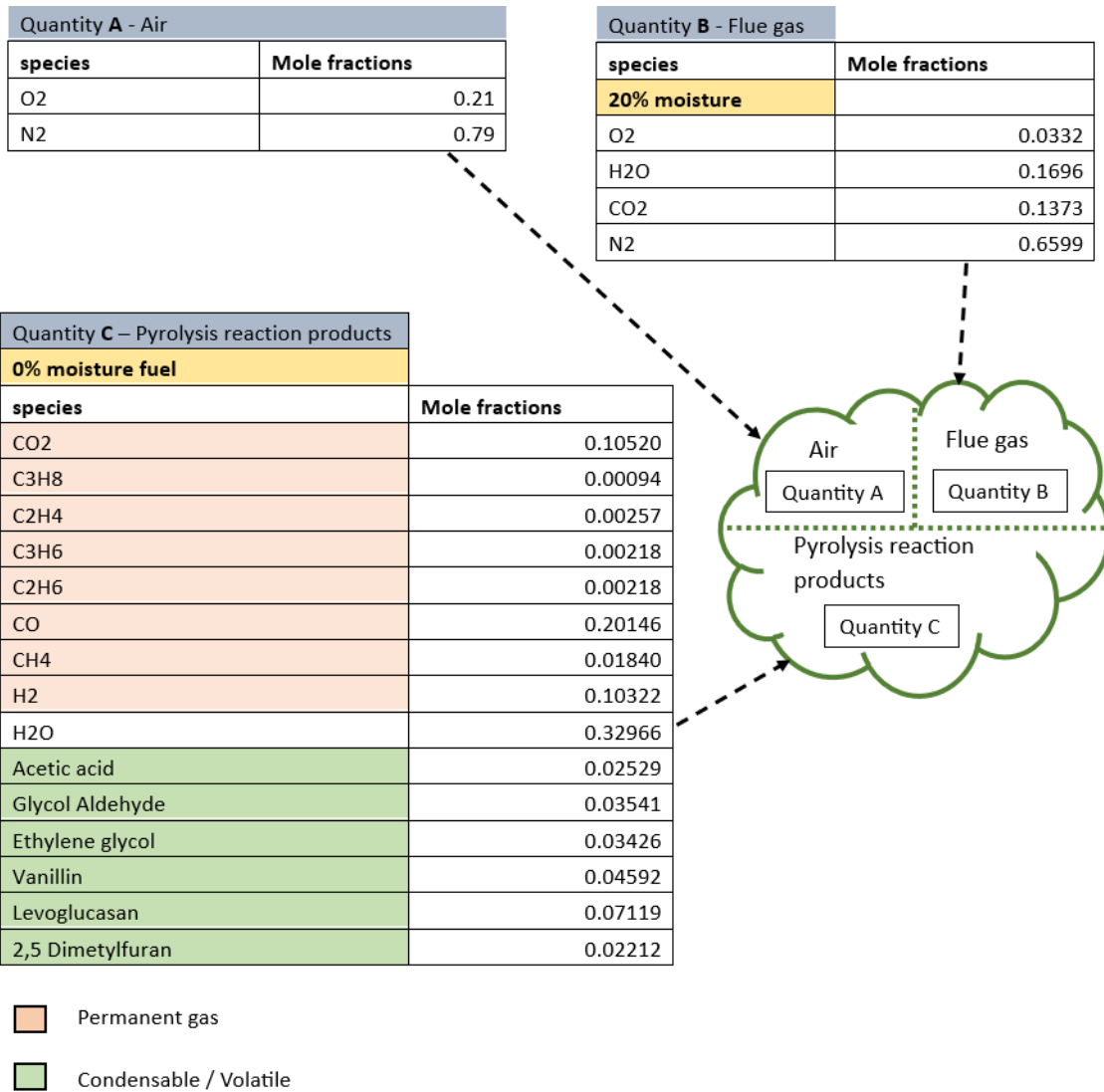


Figure 3.1: Gas mixture composition data of reactants from Bioshare that forms the explosive mixture within the endothermic reactor

## 3.2 Method

The ignition delay time provides a benchmark for the overall behavior of a combustible fuel [27]. An ignition delay analysis is performed to study and estimate the ignition limits of the explosion, as explained in the following section. As the temperature and pressure increases, the ignition delay time is expected to reduce as the mixture becomes more easy to combust. The equivalence ratio of the fuel/air mixture also changes the auto ignition characteristics. As the composition of the mixture varies to become fuel rich (i.e., as  $\phi$  varies from 0.5 to 1.5), it is expected that the auto ignition delay time will be reduced, since the concentration of fuel available to burn is higher.

As seen in the previous chapter in figure 2.2, the ignition delay criterion can be evaluated on the basis of temperature, by measuring the time taken to reach the maximum rate of change of temperature or the time taken to directly reach a reference temperature value. The latter method is chosen. The reference temperature value is set as 20% above the initial temperature of the gas mixture.

An ideal gas reactor from Cantera is used. The reactor model is defined by four state variables:  $m$ , mass of the reactor contents (kg);  $V$ , reactor volume ( $m^3$ );  $T$ , reactor temperature (K) and  $Y_k$ , mass fractions of every species  $k$  (dimensionless). The specific governing equations of the reactor are [18]:

### Global mass conservation equation

$$\frac{dm}{dt} = \sum_{in} \dot{m}_{in} - \sum_{out} \dot{m}_{out} + \dot{m}_{wall} \quad (3.2)$$

The numerical model built for ignition delay analysis assumes that the reactor is a closed system, so the rate of mass flow into and out of the system  $\sum_{in} \dot{m}_{in}$ ,  $\sum_{out} \dot{m}_{out}$  becomes zero. The reactor walls are considered chemically inert, making the final term also zero. Simplifying the above equation [18]:

$$\frac{dm}{dt} = 0 \quad (3.3)$$

where  $\dot{m}_{wall}$  is the mass generated at the reactor walls from surface phase reactions.

### Volume equation

$$\frac{dV}{dt} = \sum_w f_w A_w v_w(t)$$

where  $f_w$  is +1 or -1 indicating the facing of the wall depending on which the reactor volume increases or decreases,  $A_w$  is wall surface area and  $v_w(t)$  is the wall velocity as a function of time. Wall movement is not considered in our model, reducing the volume equation to:

$$\frac{dV}{dt} = 0 \quad (3.4)$$

The internal energy for an ideal gas in terms of temperature is defined as the summation of the specific internal energies of the individual species  $k$  as follows [18]:

### Energy equation

$$U = m \sum_k Y_k u_k(T)$$

The differential form of the total internal energy is written below, where the first term of the RHS signifies the change in specific internal energy due to the rate of change of global mass of the reactor contents, the second RHS term signifies the change in internal energy due to the change in the temperature of the system from the reaction, and the final term is the change in specific internal energy of the individual chemical species as they transform and change chemical composition during the reaction.

$$\frac{dU}{dt} = u \frac{dm}{dt} + m c_v \frac{dT}{dt} + m \sum_k u_k \frac{dY_k}{dt} \quad (3.5)$$

The species mass conservation equation gives the rate of change of mass of the individual chemical species as they transform from one component species to another in the chemical reaction. In the equation below, the first two terms in the RHS denote the flow of chemical species into and out of the system, respectively. The final term  $\dot{m}_{k,gen}$  is the rate of change in the mass of the species due to homogeneous gas phase reactions that occur in the reactor [18].

### Species mass conservation equation

$$\frac{d(mY_k)}{dt} = \sum_{in} \dot{m}_{in} Y_{k,in} - \sum_{out} \dot{m}_{out} Y_{k,out} + \dot{m}_{k,gen}$$

Considering a closed reactor, the first two terms in the RHS can be ignored to simplify the above equation as:

$$\frac{d(mY_k)}{dt} = \dot{m}_{k,gen} \quad (3.6)$$

Here,  $\dot{m}_{k,gen}$  refers to the overall mass change of any species k due to the intermediate chemical reactions that occur in the system. The same chemical species could be generated in certain intermediary reactions and consumed in other types of reactions happening in the reaction mechanism, causing a change in the overall rate of change of mass for species k.

The reactor system used in the Cantera model to study the transient phenomena of ignition delay is zero dimensional. Under steady state conditions, the reactor properties do not change with time and results in a set of algebraic equations to be solved. In the case of a transient problem, the properties vary with the evolution of time, resulting in the system to be described by a set of ODE that is specified above. The reactor object in Cantera describes this set of governing equations. To solve this set of differential equations, a 'reactor network' is used as a solver to perform time integration and solve the system of equations [18]. Usually in numerical methods of solving, the differential equations are simplified to form a set of algebraic equations that is solved in an iterative process until the solution does not vary significantly. The process ends when the variation in solution between the next to next iterative loop falls below a particular residual condition limit.

The whole simulation is carried out for 1 second, with a time step size of  $10^{-4}$  second. This corresponds to 10000 total number of time steps that the simulation runs for. The recorded properties of the gas mixture like temperature, species mass fractions, etc. that evolves with time is recorded and stored in a solution array at the end of each time step, i.e., after every  $10^{-4}$  second. The time step size has to be small enough to get an accurate numerical solution, that is a close approximation of the actual analytical solution of the governing equations. While handling a huge chemical reaction mechanism file like the one used in this model, the computational time required was high. So too small a time step size was undesirable. By iteratively running the final code for different time step sizes,  $10^{-4}$  second was fixed, as the variation in the resulting solution of ignition delay time was insignificant. This gives the desired balance between solution accuracy and computational efforts needed. The results and analysis of the ignition delay study are presented in the following chapter.

## 4 Results and Discussion

The initial temperature of the gas mixture fixed for all the results presented in this section is 923 Kelvin. The reference temperature is fixed as an increase of 20 % in the initial temperature, taking the value of 1107.6 kelvin. For the starting temperature of 923 Kelvin of the gas mixture within the reactor, ignition delay time is calculated for equivalence ratios 0.5, 1 and 1.5 in the following sections. In each of these simulation studies, the ignition delay time is also calculated for varying pressure levels.

### 4.1 For Equivalence ratio = 0.5

Figure 4.1 shows the temperature vs time plot of auto ignition phenomena within the reactor. The equivalence ratio of the composition of the gas mixture is 0.5, lean fuel mixture. As mentioned earlier in the theory chapter, the time taken by the gas mixture to reach the reference temperature of 1107.6 kelvin, indicated by the red dot on each pressure curve as seen in the plot below, is recorded as their respective ignition delay times. The horizontal dotted black line indicates the reference temperature.

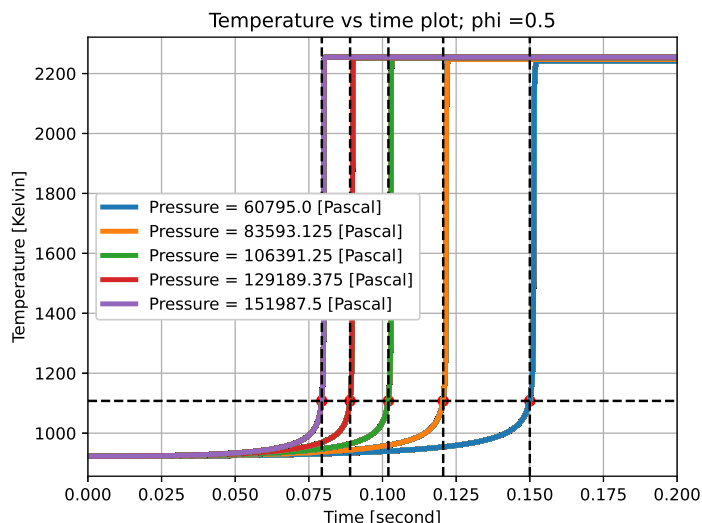


Figure 4.1: *Temperature vs time plot for given gas mixture with 0.5 equivalence ratio*

From the graph, it is observed that the ignition delay time reduces as the pressure increases. The time taken for the mixture to spontaneously ignite reduces as the pressure of the reactor system increases. The final temperature reached by the explosive mixture at the end of ignition also increases with the increase in temperature. The specific initial and final temperature and pressure values for every pressure level are recorded in the appendix B.

The disappearance rate of the reactant species  $CH_4$  and the formation of the product species  $H_2O$  is plotted in the figure 4.2 below. The variation in the mole fraction of the species is plotted for the highest pressure level, 151987.5 Pa. The instant of time at which the species concentration peaks/drops corresponds to the ignition phenomenon occurring as a result of the chain branching reactions. The recorded time for the increase / decrease in product / reactant can be seen to coincide with the ignition delay time in the temperature vs time plot 4.1, as expected.

The rate of change in the concentration of reactant species is less than that of the product species. The nature of the curves are exponential, which agrees with the empirical power law type of reaction rate expression, as seen in the theory chapter. This nature of the reaction indicates normal chemical kinetics.

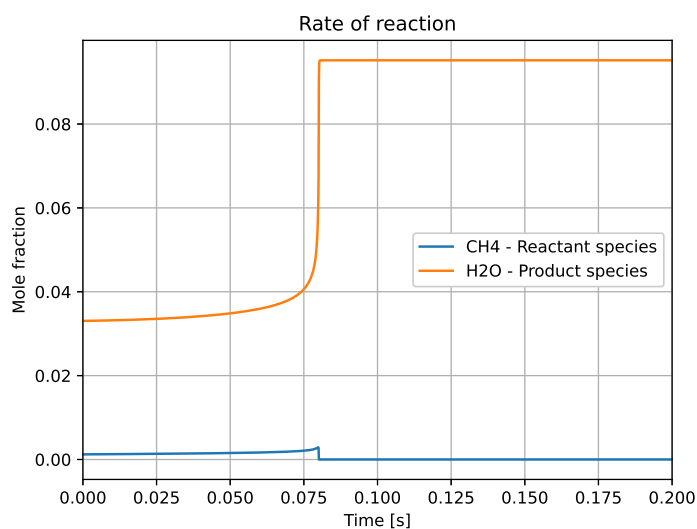


Figure 4.2: Rate of change of mole fraction of reactant and product species when equivalence ratio = 0.5

The plot in figure 4.3 below maps the change in the mole fraction of the radical species OH, for the equivalence ratio 0.5 and at the initial pressure level 151987.5 Pa. The sudden peak build up of the radicals indicates the ignition phenomena corresponding to the chain branching reactions. The ignition time value matches the observed ignition delay time for the same conditions in the previous plots. Once the radical concentration reaches its peak, it is transformed and consumed in chain branching and chain propagation type reactions, thus reducing its concentration.

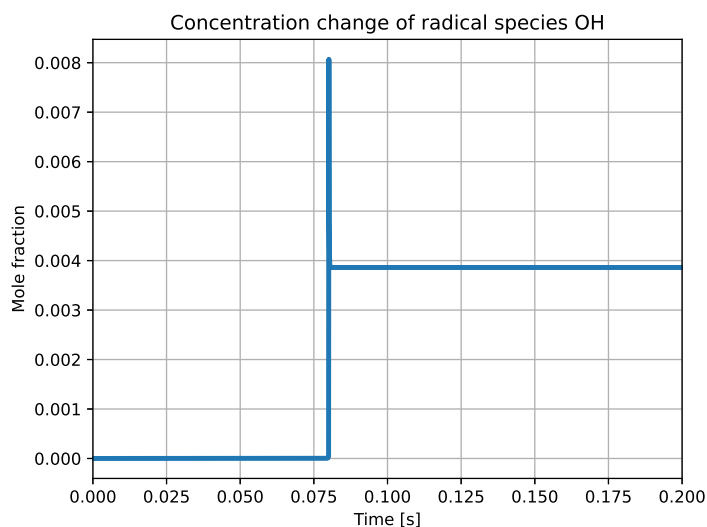


Figure 4.3: Rate of change of mole fraction of the radical species OH when equivalence ratio = 0.5

## 4.2 For Equivalence ratio = 1.0

Similar behavior for ignition delay is observed when the equivalence ratio is changed to 1. The ignition delay time reduces as the pressure level increases. Comparing the plot below with the previous plot 4.1, we can observe that the ignition delay time decreases as the equivalence ratio increases. The final temperature reached after ignition also increases as the pressure increases. The final temperatures reached at the end of ignition with this stoichiometric mixture composition is the highest when compared to the final temperatures reached for the equivalence ratio values 0.5 and 1.5, as seen in B

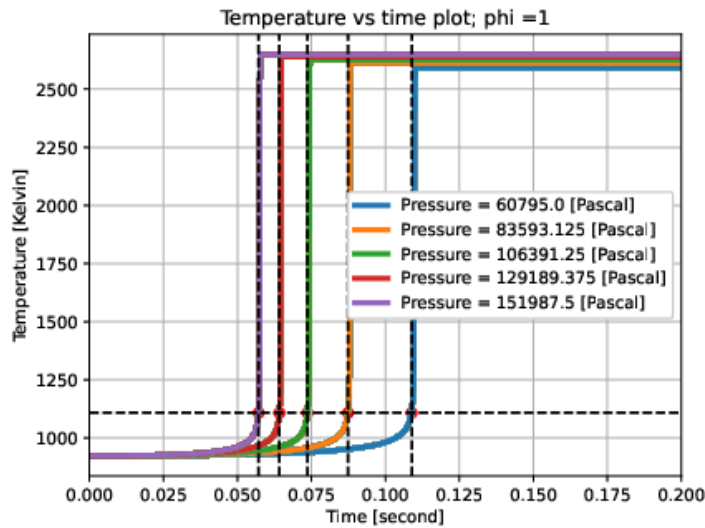


Figure 4.4: *Temperature vs time plot for given gas mixture with 1.0 equivalence ratio*

As seen in the previous reaction rate plot 4.2, the rate of formation and consumption of the product and the reactant species exhibit a similar behavior. The rate change of the species is mapped for the same reactant species  $CH_4$  and product species  $H_2O$  at the pressure level 151987.5 Pa. The reaction rate changes the most during ignition chain branching reactions. This time recorded corresponds to the same ignition delay time from 4.4 plot for the pressure level 151987.5 Pa. The build up of the radical species correspond to the ignition

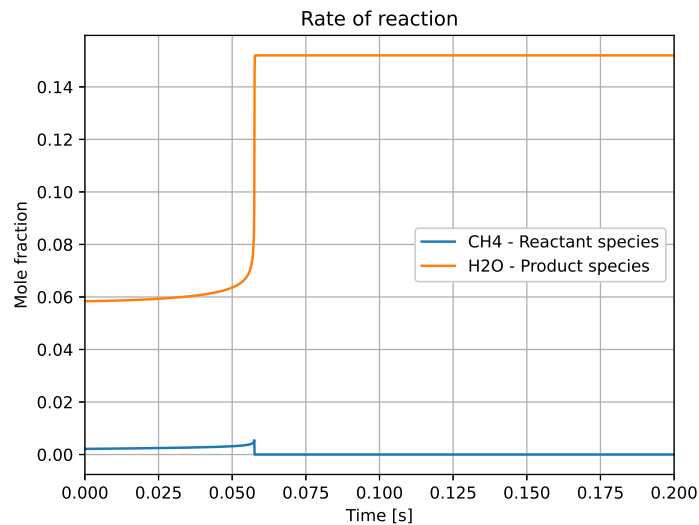


Figure 4.5: *Rate of change of mole fraction of reactant and product species when equivalence ratio = 1.0*

phenomena for the gas mixture at equivalence ratio 1 and initial pressure level of 151987.5 Pa.

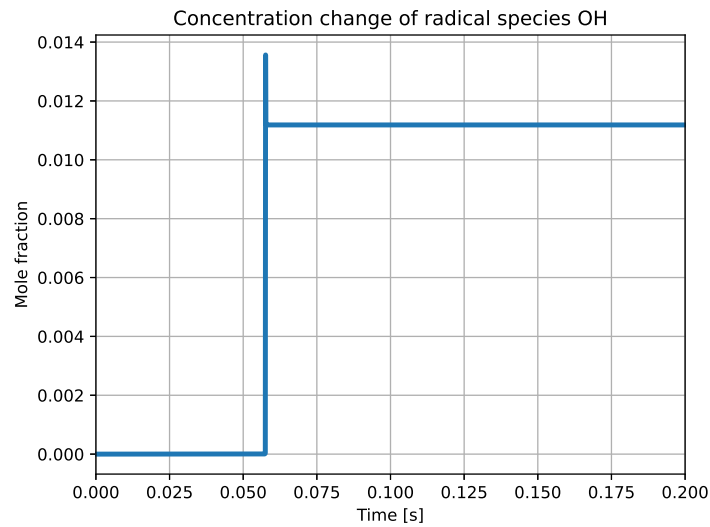


Figure 4.6: Rate of change of mole fraction of the radical species OH when equivalence ratio = 1.0

### 4.3 For Equivalence ratio = 1.5

A similar behavior of ignition delay time is observed when the equivalence ratio changes to 1.5, becoming fuel rich. The ignition delay time recorded is the least compared to the previous ignition delay results, as expected, since the fuel concentration increases.

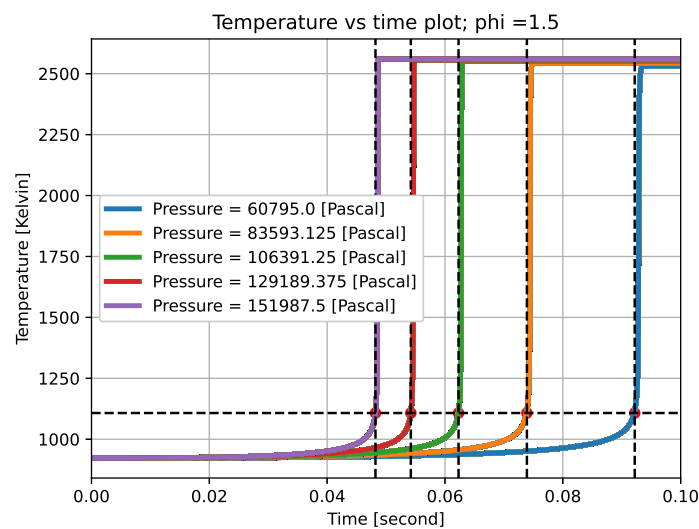


Figure 4.7: Temperature vs time plot for given gas mixture with 1.5 equivalence ratio

The reaction rate behavior similar to the previous cases is observed for the 1.5 equivalence ratio as well in the plot 4.8 below.

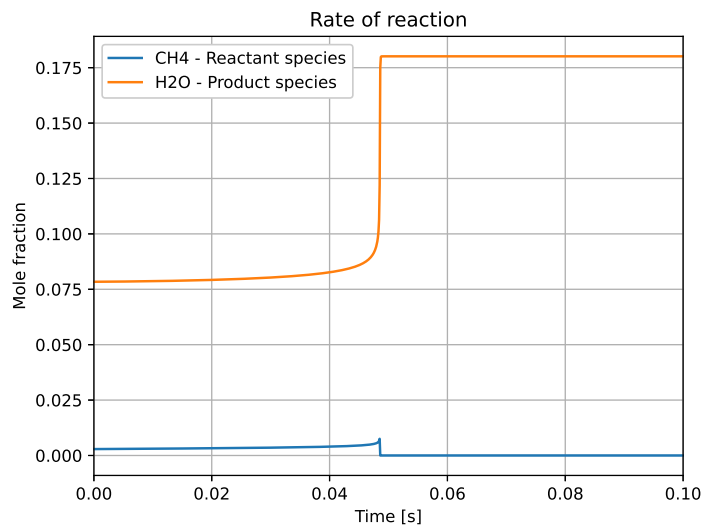


Figure 4.8: Rate of change of mole fraction of reactant and product species when equivalence ratio = 1.5

The plot below 4.9 shows the build up of the radical species OH corresponding to the ignition phenomena for an equivalence ratio of 1.5 and an initial pressure level of 151987.5 Pa.

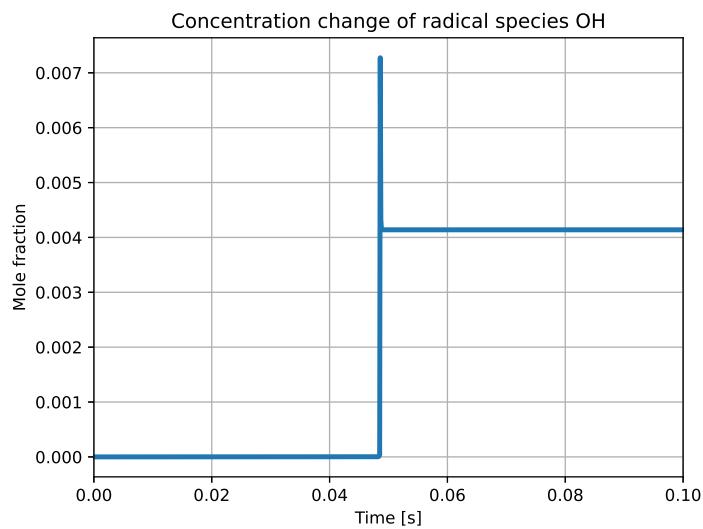
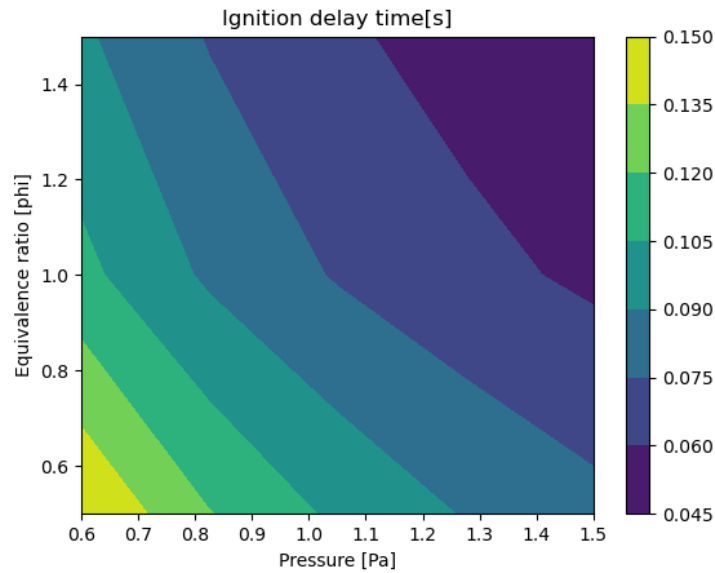


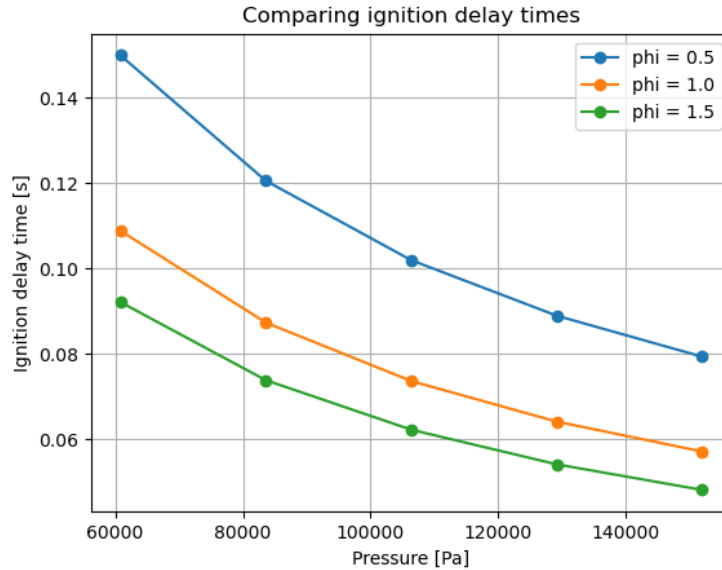
Figure 4.9: Rate of change of mole fraction of the radical species OH when equivalence ratio = 1.5

## 4.4 Ignition delay comparison study

The ignition delay times for the varying equivalence ratio values seen previously is compared in the following two plots. The ignition delay time decreases as the pressure increases and decreases as equivalence ratio value increases.



(a) Ignition delay contour plot for initial temperature 923 K



(b) Ignition delay time curves for varying equivalence ratios ( $\phi$ ) at values 0.5, 1, 1.5

Figure 4.10: Ignition delay time behaviour

## 4.5 Temperature dependency

The ignition delay time period can be seen to depend exponentially on the reciprocal temperature [20] :

$$\tau = A.exp(B/T) \quad (4.1)$$

From this expression, the logarithm of the ignition delay time period  $\tau$  should have a linear relationship with the reciprocal of the temperature  $1/T$ , as can be seen in the plot below. The Arrhenius law gives the temperature dependence of the elementary reactions in the reaction mechanism [20]. The simulation of the plot

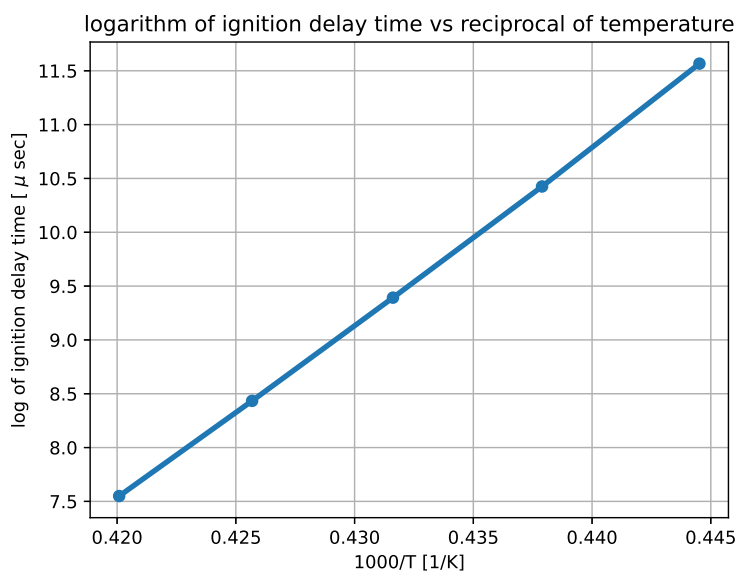


Figure 4.11: *Logarithm of ignition delay time vs temperature inverse*

4.11 was carried out by setting the pressure at 1 bar and varying the temperature at 5 equally spaced levels, between 650 °C and 850 °C.

The results presented above used a time step size of  $1e^{-4}$  seconds. The same simulation study was carried out for a smaller time step size of  $1e^{-5}$  second. The corresponding ignition delay time values, presented in appendix C, show similar results as those with  $1e^{-4}$  second time step size. Thus, the results found in this thesis study can be validated to be independent of the time step size.

## 5 Conclusion

This thesis investigated the limits of the potential chemical explosion within the gasification reactor. The basics of the underlying reaction mechanism were studied. The chemical kinetics was interpreted and modeled using the open-source software tool Cantera. A time step size of  $1e^{-4}$  second is fixed for the numerical model. The results did not vary significantly with further refinement of the time step and were independent of the selected time step size. The solution accuracy provided by the  $1e^{-4}$  second time step was found to give satisfactory results for the purpose of the model. The computational time required to run the heavy Pelucchi reaction mechanism file was a major challenging factor while setting up and running the model. Key findings from the simulation study are as follows:

- As the temperature of the initial gas mixture increases, the ignition delay time of the explosion is reduced.
- As the pressure of the initial mixture increases, the ignition delay time of the explosion is reduced.
- As the equivalence ratio of the mixture increases, the ignition delay time of the explosion is reduced.

From the numerical model setup, spontaneous auto ignition of the mixture was observed at an initial temperature of around 600 °C. The reactor environment is expected to easily cross this temperature, thereby increasing the incidence of chemical explosion. During the combustion reaction within the boiler, its temperature would approximately be around 1000 °C or higher. The bed material transferred from this high temperature boiler environment to the gasification reactor will subsequently also increase the reactor temperature proportionally. Keeping this in mind, further study of the safety design considerations of the gasification reactor is the way forward.

The understanding of ignition delay from this thesis work also has wider applications outside of the thesis objective. The ignition delay is an important parameter in the combustion analysis of compression ignition engines. Controlling or reducing ignition delay is an effective way to improve the fuel economy and thermal efficiency of engines and reduce pollutant emissions.

### 5.1 Future work

This research provides a foundation for testing and evaluating the chemical explosion limits within the gasification reactor. Future work could include the development of a calculation model to estimate the maximum pressure increase during the vented gas explosion within the reactor. The ignition delay simulation model built in this thesis work is 0-dimensional and required only the input of thermodynamic properties and reaction mechanism file of the participating species in Cantera. A 0-dimensional model is insufficient for the study of pressure increase.

The scope of this study could be extended to implement a 1-dimensional flame model in Cantera. This can be used to calculate the burning velocity of the propagating flame front during the explosion within the reactor to see how fast the propagation occurs within the gasification reactor under specified conditions. An additional input of the transport properties has to be estimated and formulated for the Pelucchi reaction mechanism file to model the 1-dimensional flame model.

## References

- [1] *The Human Fingerprint on Greenhouse Gases*. URL: <https://www.un.org/en/global-issues/climate-change>.
- [2] *What Are the Effects of Climate Change?* URL: <https://www.nrdc.org/stories/what-are-effects-climate-change>.
- [3] *Climate action*. URL: <https://www.unep.org/topics/climate-action>.
- [4] *Implementation of bioenergy in Sweden – 2021 update*. 2021. URL: [https://www.ieabioenergy.com/wp-content/uploads/2021/11/CountryReport2021\\_Sweden\\_final.pdf](https://www.ieabioenergy.com/wp-content/uploads/2021/11/CountryReport2021_Sweden_final.pdf).
- [5] *Swedes use a lot of energy – yet, emissions are low. The key? Renewable energy*. Last accessed on July 6, 2023. URL: <https://sweden.se/climate/sustainability/energy-use-in-sweden>.
- [6] *Bioenergy, a sustainable solution*. IEA Bioenergy. URL: <https://www.ieabioenergy.com/bioenergy-a-sustainable-solution/>.
- [7] *Bioenergy*. URL: <https://www.iea.org/energy-system/renewables/bioenergy#tracking>.
- [8] *Biomass explained*. U.S. Energy Information Administration. URL: <https://www.eia.gov/energyexplained/biomass/>.
- [9] Şebnem Yılmaz Balaman. “Chapter 1 - Introduction to Biomass—Resources, Production, Harvesting, Collection, and Storage”. *Decision-Making for Biomass-Based Production Chains*. Ed. by Şebnem Yılmaz Balaman. Academic Press, 2019, pp. 1–23. ISBN: 978-0-12-814278-3. DOI: <https://doi.org/10.1016/B978-0-12-814278-3.00001-7>. URL: <https://www.sciencedirect.com/science/article/pii/B9780128142783000017>.
- [10] *Land use sector*. URL: [https://climate.ec.europa.eu/eu-action/land-use-sector\\_en](https://climate.ec.europa.eu/eu-action/land-use-sector_en).
- [11] Jannick H. Schmidt, Bo P. Weidema, and Miguel Brandão. A framework for modelling indirect land use changes in Life Cycle Assessment. *Journal of Cleaner Production* **99** (2015), 230–238. ISSN: 0959-6526. DOI: <https://doi.org/10.1016/j.jclepro.2015.03.013>. URL: <https://www.sciencedirect.com/science/article/pii/S0959652615002309>.
- [12] Alan Matthews. Carbon removal certification and carbon farming (2023). DOI: <https://doi.org/10.1016/j.jclepro.2015.03.013>. URL: <http://capreform.eu/carbon-removal-certification-and-carbon-farming/>.
- [13] *National emissions reported to the UNFCCC and to the EU under the Governance Regulation, 2025*. Version 3.0. European Environment Agency (EEA), 2021. URL: <https://www.eea.europa.eu/en/analysis/indicators/greenhouse-gas-emissions-from-land/eu-emissions-and-removals?activeTab=570bee2d-1316-48cf-adde-4b640f92119b>.
- [14] *Sustainable Carbon Cycles*. EUROPEAN COMMISSION, 2021. URL: [https://climate.ec.europa.eu/system/files/2021-12/com\\_2021\\_800\\_en\\_0.pdf](https://climate.ec.europa.eu/system/files/2021-12/com_2021_800_en_0.pdf).
- [15] *What Is CHP?* United States Environmental Protection Agency, 2023. URL: <https://www.epa.gov/chp/what-chp>.
- [16] “Fluidized bed”. Accessed on 23rd July 2023. URL: [https://www.chemeurope.com/en/encyclopedia/Fluidized\\_bed.html](https://www.chemeurope.com/en/encyclopedia/Fluidized_bed.html).
- [17] Nikhil Chakravarthy Ramesh Chandragiri. Design of Fermenter and Fluidized Bed Bioreactor. *International Journal of Chemical Sciences* **21(1)** (2023). ISSN: 0972-768X. DOI: 10.37532/0972-768X.2023.21(1).430. URL: <https://www.tsijournals.com/articles/design-of-fermenter-and-fluidized-bed-bioreactor.pdf>.
- [18] David G. Goodwin et al. *Cantera: An Object-oriented Software Toolkit for Chemical Kinetics, Thermodynamics, and Transport Processes*. <https://www.cantera.org>. Version 2.6.0. 2022. DOI: 10.5281/zenodo.6387882.
- [19] Matteo Pelucchi et al. Detailed kinetics of substituted phenolic species in pyrolysis bio-oils. *React. Chem. Eng.* **4** (3 2019), 490–506. DOI: 10.1039/C8RE00198G. URL: <http://dx.doi.org/10.1039/C8RE00198G>.
- [20] R.W.Dibble J.Warnatz U.Mass. *Combustion*. Springer, 2006. ISBN: 978-3-540-25992-3.
- [21] S.Andersson et al. “Combustion engineering (MEN031) notes”. Department of Energy and Environment, Chalmers University of Technology, Gothenburg, Sweden, 2020.
- [22] J.P.Mmbag R.E. Hayes. *Introduction to Chemical Reactor Analysis, Second edition*. CRC Press, 2013. ISBN: 13: 978-1-4665-8053-4.

- [23] “Arrhenius Equation”. URL: <https://chemistrytalk.org/arrhenius-equation/>.
- [24] Kenneth B. Bischoff Gilbert F. Froment and Juray De Wilde. *Chemical Reactor Analysis and Design, 3rd Edition*. Wiley, 2011. ISBN: 978-1-118-13653-9.
- [25] James G. Speight. “Chapter 10 - Combustion of hydrocarbons”. *Handbook of Industrial Hydrocarbon Processes (Second Edition)*. Ed. by James G. Speight. Second Edition. Boston: Gulf Professional Publishing, 2020, pp. 421–463. ISBN: 978-0-12-809923-0. DOI: <https://doi.org/10.1016/B978-0-12-809923-0.00010-2>. URL: <https://www.sciencedirect.com/science/article/pii/B9780128099230000102>.
- [26] Tomio Okawa et al. “3-Fundamentals for power engineering”. *Fundamentals of Thermal and Nuclear Power Generation*. Ed. by Yasuo Koizumi, Tomio Okawa, and Shoji Mori. Vol. 1. JSME Series in Thermal and Nuclear Power Generation. Elsevier, 2021, pp. 77–226. ISBN: 978-0-12-820733-8. DOI: <https://doi.org/10.1016/B978-0-12-820733-8.00003-0>. URL: <https://www.sciencedirect.com/science/article/pii/B9780128207338000030>.
- [27] “series : Computer Aided Chemical Engineering”. *Mathematical Modelling of Gas-Phase Complex Reaction Systems: Pyrolysis and Combustion*. Ed. by Tiziano Faravelli, Flavio Manenti, and Eliseo Ranzi. Vol. 45. Elsevier, 2019, pp. xvii–xx. DOI: <https://doi.org/10.1016/B978-0-444-64087-1.09990-3>. URL: <https://www.sciencedirect.com/science/article/pii/B9780444640871099903>.

# A Appendix

```
1
2 import cantera as ct
3 import numpy as np
4 import matplotlib.pyplot as plt
5
6 # Input gas reaction mechanism file
7 gas = ct.Solution('kinetics.CHEMKIN.yaml')
8
9 # Pressure range and Initial temperature values
10 P_minimum = 0.6 * ct.one_atm # [Pascal]
11 P_maximum = 1.5 * ct.one_atm # [Pascal]
12
13 # Pressure range split into 5 levels
14 n = 5
15 Pressure_range = np.linspace (P_minimum,P_maximum,n)
16
17 # Pressure = 1*ct.one_atm # [Pascal]
18 Temperature = 650 + 273 # [Kelvin]
19
20 # Reference temperature fixed by user to calculate ignition delay time
21 T_ref = 1.2 * Temperature # [Kelvin]
22
23 # Quantity A (air)
24 A = ct.Quantity(gas)
25 A.X = ' O2:0.21, N2:0.79 '
26
27
28 # Quantity B (flue gas) - fluidization gas for reactor
29 B = ct.Quantity(gas)
30 # 1st composition (20% moisture) under Flue gas from Bioshare
31 B.X = ' O2:0.03322, H2O:0.1696, CO2:0.1373, N2:0.6599 '
32
33 # 2nd composition under Flue gas from Bioshare
34 #B.TPX = T, ct.one_atm, ' O2:0.02916, H2O:0.2711, CO2:0.1205, N2:0.5792 '
35
36 # 3rd composition under Flue gas from Bioshare
37 #B.TPX = T, ct.one_atm, ' O2:0.02395, H2O:0.4012, CO2:0.09899, N2:0.4758 '
38
39 # Quantity C (Pyrolysis reaction products)
40 # 1st composition (0% moisture) under Pyrolysis reactants from Bioshare
41 C = ct.Quantity(gas)
42 C.X = ' CO2:0.10520, C3H8:0.00094, C2H4:0.00257, C3H6:0.00218, C2H6
         :0.00218, CO:0.20146, CH4:0.01840, H2:0.10322, H2O:0.32966, CH3CO2H
         :0.02529, CH2OHCHO:0.03541, CH2OHCH2OH:0.03426, VANILLIN:0.04592,
         C6H10O5:0.07119, DMF:0.02212 '
43
44 # Mixed state of all 3 Quantities - M
45 M = A + B + C
46
47 # FOR EQUIVALENCE RATIO = 0.5
48 phi = 0.5
49 # Ignition delay array
50 ignition_delay_a = []
```

```

51
52 print ('Equivalence ratio (phi) = ', phi, ': \n')
53
54 for Pressure in Pressure_range:
55
56     # display Initial states
57     print ('Initial set Pressure [Pa] =', Pressure, ' \nInitial set
        Temperature [K] = ', Temperature)
58
59     # Initialising the gas object with:
60     gas.X = M.X # Composition
61     gas.TP = Temperature, Pressure # Temperature and Pressure
62
63     gas.set_equivalence_ratio( phi, fuel=' O2:0.03322, H2O:0.49926, CO2
        :0.2425 , N2:0.6599, C3H8:0.00094, C2H4:0.00257, C3H6:0.00218, C2H6
        :0.00218, CO:0.20146, CH4:0.01840, H2:0.10322, CH3CO2H:0.02529,
        CH2OHCHO:0.03541, CH2OHCH2OH:0.03426, VANILLIN:0.04592, C6H10O5
        :0.07119, DMF:0.02212 ', oxidizer=' O2:0.21, N2:0.79 ', basis="mole
        ")
64
65     # Total time in seconds the simulation runs for = total number of time
        steps * size of each time step
66     total_time_steps = 10000 # Total number of time steps
67     step_size = 1e-4 # size of each time step
68
69     # Creating an 0D ideal gas reactor filled with gas object as defined
        above
70     reactor = ct.IdealGasReactor(gas)
71
72     # reactor object is defined within a Reactor network
73     reactor_network = ct.ReactorNet([reactor])
74
75     # Starting value of time step = 0
76     time_step = 0 # time step
77
78     # Solution array
79     states = ct.SolutionArray(gas, extra='time')
80
81     # Loop to calculate
82
83     for i in range(total_time_steps+1):
84
85         # time_step starts from [0] goes till [total_time_steps-1] ;
86         time_step += step_size # incrementing time step with the specified
            time step size
87
88         # Reactor
89         reactor_network.advance(time_step)
90
91         # Change in values of the thermodynamic states in the reactor at
            every time step
92         states.append(reactor.thermo.state, time = time_step)
93
94         # ignition delay time calculation based on reference temperature
95         while (states.T[i] >= T_ref) and (states.T[i-1] < T_ref):
96             ignition_delay_a.append(states.time[i])

```

```

97         break
98     # plot
99     fig1 = plt.figure(1)
100
101     plt.plot(states.time, states.T, lw=3 )
102     # display final states
103     print ('Final Pressure reached [Pa] =', states.P[i], ' \nFinal
        Temperature reached [K] = ', states.T[i],'\n')
104
105     # plot
106     y = [T_ref]
107     plt.title('Temperature vs time plot; phi = ' + str(phi) )
108     plt.xlabel('Time [second]')
109     plt.ylabel('Temperature [Kelvin]')
110     plt.xlim(0,0.2)
111     plt.grid('on')
112     plt.legend(['Pressure = ' + str(Pressure) + ' [Pascal]' for Pressure in
        Pressure_range])
113     plt.axhline(y=T_ref, color='black', linestyle='--')
114     for id in ignition_delay_a:
115         plt.axvline(x=id, color='black', linestyle='--')
116         plt.scatter(id, T_ref, color='red', marker = 'o')
117     # saving plot
118     image_format = 'eps' # e.g .png, .svg, etc.
119     image_name = 'image1.eps'
120     fig1.savefig(image_name, format=image_format)
121
122     # reaction rate plot
123     fig2 = plt.figure(2)
124     reactant = "CH4"
125     product = "H2O"
126     plt.plot(states.time, states(reactant).X )
127     plt.plot(states.time, states(product).X )
128     plt.xlim(0,0.2)
129     plt.grid('on')
130     plt.title('Rate of reaction')
131     plt.xlabel('Time [s]')
132     plt.ylabel('Mole fraction')
133     plt.legend(['CH4 - Reactant species','H2O - Product species'])
134     plt.show()
135     image_format = 'eps' # e.g .png, .svg, etc.
136     image_name = 'image2.eps'
137     fig2.savefig(image_name, format=image_format)
138
139     # Excel file recording all the thrmodynamic states for final pressure study
        value 151987.5 Pa
140     states.write_csv('file_0.5.csv')
141
142     # display ignition delay time
143     print('Ignition delay time [seconds] =', ignition_delay_a, 'where
        equivalence ratio (phi)=', phi)
144     %% FOR EQUIVALENCE RATIO = 1
145
146     phi = 1
147     # Ignition delay array
148     ignition_delay_b = []

```

```

149
150 print ('\n \nEquivalence ratio (phi) = ', phi, ': \n')
151 for Pressure in Pressure_range:
152
153     # display Initial states
154     print ('Initial set Pressure [Pa] =', Pressure, ' \nInitial set
        Temperature [K] = ', Temperature)
155
156     # Initialising the gas object with:
157     gas.X = M.X # Composition
158     gas.TP = Temperature, Pressure # Temperature and Pressure
159
160     gas.set_equivalence_ratio( phi, fuel=' O2:0.03322, H2O:0.49926, CO2
        :0.2425 , N2:0.6599, C3H8:0.00094, C2H4:0.00257, C3H6:0.00218, C2H6
        :0.00218, CO:0.20146, CH4:0.01840, H2:0.10322, CH3CO2H:0.02529,
        CH2OHCHO:0.03541, CH2OHCH2OH:0.03426, VANILLIN:0.04592, C6H10O5
        :0.07119, DMF:0.02212 ', oxidizer=' O2:0.21, N2:0.79 ', basis="mole
        ")
161
162     # Total time in seconds the simulation runs for = total number of time
        steps * size of each time step
163     total_time_steps = 10000 # Total number of time steps
164     step_size = 1e-4 # size of each time step
165
166     # Creating an OD ideal gas reactor filled with gas object as defined
        above
167     reactor = ct.IdealGasReactor(gas)
168
169     # reactor object is defined within a Reactor network
170     reactor_network = ct.ReactorNet([reactor])
171
172     # Starting value of time step = 0
173     time_step = 0 # time step
174
175     # Solution array
176     states = ct.SolutionArray(gas, extra='time')
177
178     # Loop to calculate
179
180     for i in range(total_time_steps+1):
181
182         # time_step starts from [0] goes till [total_time_steps-1] ;
183         time_step += step_size # incrementing time step with the specified
            time step size
184
185         # Reactor
186         reactor_network.advance(time_step)
187
188         # Change in values of the thermodynamic states in the reactor at
            every time step
189         states.append(reactor.thermo.state, time = time_step)
190
191         # ignition delay time calculation based on reference temperature
192         while (states.T[i] >= T_ref) and (states.T[i-1] < T_ref):
193             ignition_delay_b.append(states.time[i])
194             break

```

```

195         # plot
196         fig3 = plt.figure(3)
197
198         plt.plot(states.time, states.T, lw=3 )
199         # display final states
200         print ('Final Pressure reached [Pa] =', states.P[i], ' \nFinal
           Temperature reached [K] = ', states.T[i], '\n')
201
202     # plot
203     y = [T_ref]
204     plt.title('Temperature vs time plot; phi = ' + str(phi) )
205     plt.xlabel('Time [second]')
206     plt.ylabel('Temperature [Kelvin]')
207     plt.xlim(0,0.2)
208     plt.grid('on')
209     plt.legend(['Pressure = ' + str(Pressure) + ' [Pascal]' for Pressure in
           Pressure_range])
210     plt.axhline(y=T_ref, color='black', linestyle='--')
211     for id in ignition_delay_b:
212         plt.axvline(x=id, color='black', linestyle='--')
213         plt.scatter(id, T_ref, color='red', marker = 'o')
214     # saving plot
215     image_format = 'eps' # e.g .png, .svg, etc.
216     image_name = 'image3.eps'
217     fig3.savefig(image_name, format=image_format)
218
219     # reaction rate plot
220     fig4 = plt.figure(4)
221     reactant = "CH4"
222     product = "H2O"
223     plt.plot(states.time, states(reactant).X )
224     plt.plot(states.time, states(product).X )
225     plt.grid('on')
226     plt.title('Rate of reaction')
227     plt.xlabel('Time [s]')
228     plt.ylabel('Mole fraction')
229     plt.xlim(0,0.2)
230     plt.legend(['CH4 - Reactant species','H2O - Product species'])
231     plt.show()
232     image_format = 'eps' # e.g .png, .svg, etc.
233     image_name = 'image4.eps'
234     fig4.savefig(image_name, format=image_format)
235     # Excel file recording all the thrmodynamic states for final pressure study
           value 151987.5 Pa
236     #states.write_csv('file_1.csv')
237     # display ignition delay time
238     print('Ignition delay time [seconds] =', ignition_delay_b, 'where
           equivalence ratio (phi)=', phi)
239
240     ### FOR EQUIVALENCE RATIO = 1.5
241     phi = 1.5
242     # Ignition delay array
243     ignition_delay_c = []
244
245     print ('\n \nEquivalence ratio (phi) = ', phi, ': \n')
246     for Pressure in Pressure_range:

```

```

247 # display Initial states
248 print ('Initial set Pressure [Pa] =', Pressure, ' \nInitial set
      Temperature [K] = ', Temperature)
249
250 # Initialising the gas object with:
251 gas.X = M.X # Composition
252 gas.TP = Temperature, Pressure # Temperature and Pressure
253
254 gas.set_equivalence_ratio( phi, fuel=' O2:0.03322, H2O:0.49926, CO2
      :0.2425 , N2:0.6599, C3H8:0.00094, C2H4:0.00257, C3H6:0.00218, C2H6
      :0.00218, CO:0.20146, CH4:0.01840, H2:0.10322, CH3CO2H:0.02529,
      CH2OHCHO:0.03541, CH2OHCH2OH:0.03426, VANILLIN:0.04592, C6H10O5
      :0.07119, DMF:0.02212 ', oxidizer=' O2:0.21, N2:0.79 ', basis="mole
      ")
255
256 # Total time in seconds the simulation runs for = total number of time
      steps * size of each time step
257 total_time_steps = 10000 # Total number of time steps
258 step_size = 1e-4 # size of each time step
259
260 # Creating an 0D ideal gas reactor filled with gas object as defined
      above
261 reactor = ct.IdealGasReactor(gas)
262
263 # reactor object is defined within a Reactor network
264 reactor_network = ct.ReactorNet([reactor])
265
266 # Starting value of time step = 0
267 time_step = 0 # time step
268
269 # Solution array
270 states = ct.SolutionArray(gas, extra='time')
271
272 # Loop to calculate
273
274 for i in range(total_time_steps+1):
275
276     # time_step starts from [0] goes till [total_time_steps-1] ;
277     time_step += step_size # incrementing time step with the specified
      time step size
278
279     # Reactor
280     reactor_network.advance(time_step)
281
282     # Change in values of the thermodynamic states in the reactor at
      every time step
283     states.append(reactor.thermo.state, time = time_step)
284
285     # ignition delay time calculation based on reference temperature
286     while (states.T[i] >= T_ref) and (states.T[i-1] < T_ref):
287         ignition_delay_c.append(states.time[i])
288         break
289
290     # plot
291     fig5 = plt.figure(5)
292
293     plt.plot(states.time, states.T, lw=3 )

```

```

293     plt.xlim(0,0.1)
294     # display final states
295     print ('Final Pressure reached [Pa] =', states.P[i], ' \nFinal
        Temperature reached [K] = ', states.T[i],'\n')
296
297     # plot
298     y = [T_ref]
299     plt.title('Temperature vs time plot; phi = ' + str(phi) )
300     plt.xlabel('Time [second]')
301     plt.ylabel('Temperature [Kelvin]')
302     plt.grid('on')
303     plt.legend(['Pressure = ' + str(Pressure) + ' [Pascal]' for Pressure in
        Pressure_range])
304     plt.axhline(y=T_ref, color='black', linestyle='--')
305     for id in ignition_delay_c:
306         plt.axvline(x=id, color='black', linestyle='--')
307         plt.scatter(id, T_ref, color='red', marker = 'o')
308     # saving plot
309     image_format = 'eps' # e.g .png, .svg, etc.
310     image_name = 'image5.eps'
311     fig5.savefig(image_name, format=image_format)
312
313     # reaction rate plot
314     fig6 = plt.figure(6)
315     reactant = "CH4"
316     product = "H2O"
317     plt.plot(states.time, states(reactant).X )
318     plt.plot(states.time, states(product).X )
319     plt.xlim(0,0.1)
320     plt.grid('on')
321     plt.title('Rate of reaction')
322     plt.xlabel('Time [s]')
323     plt.ylabel('Mole fraction')
324     plt.legend(['CH4 - Reactant species','H2O - Product species'])
325     plt.show()
326
327     image_format = 'eps' # e.g .png, .svg, etc.
328     image_name = 'image6.eps'
329     fig6.savefig(image_name, format=image_format)
330     # Excel file recording all the thrmodynamic states for final pressure study
        value 151987.5 Pa
331     states.write_csv('file_1.5.csv')
332     # display ignition delay time
333     print('Ignition delay time [seconds] =', ignition_delay_c, 'where
        equivalence ratio (phi)=', phi)

```

## B Appendix

Recorded Temperature, pressure and ignition delay values for the combustible mixture at each pressure level [60795.0 Pa, 83593.125 Pa, 106391.25 Pa, 129189.375 Pa and 151987.5 Pa] for varying equivalence ratios with the initial set temperature of 923 Kelvin and time step size  $1e^{-4}$  seconds are shown below.



Initial Temp = 923 K

0.1206000000000243, 0.1020000000000019, 0.08900000000000152, 0.07940000000000125] where equivalence ratio ( $\phi$ )= 0.5		0.07390000000000109, 0.06230000000000076, 0.054200000000000526, 0.048200000000000354] where equivalence ratio ( $\phi$ )= 1.5
---	--	--

## C Appendix

Recorded ignition delay values for the combustible mixture at each pressure level [60795.0 Pa, 83593.125 Pa, 106391.25 Pa, 129189.375 Pa and 151987.5 Pa] for varying equivalence ratios but with time step size  $1e^{-5}$  seconds are shown below. The ignition delay time recorded is observed not to vary significantly when compared to the previous results with a bigger time step size of  $1e^{-4}$  seconds.

Initial set Temperature [K] = 923

Initial set pressure [Pa]	Equivalence ratio ( $\phi$ ) = 0.5	Equivalence ratio ( $\phi$ ) = 1.0	Equivalence ratio ( $\phi$ ) = 1.5
60795.0	0.14991000000000915	0.10881999999999051	0.09211999999999698
83593.125	0.12051999999998597	0.08731999999998845	0.0738500000000407
106391.25	0.1019299999999318	0.0737000000000412	0.0622800000000084
129189.375	0.088969999999982	0.06419000000000781	0.05420000000005924
151987.5	0.0793400000000194	0.05713000000000682	0.048190000000004084

DEPARTMENT OF Mechanics and Maritime Sciences  
CHALMERS UNIVERSITY OF TECHNOLOGY  
Gothenburg, Sweden  
[www.chalmers.se](http://www.chalmers.se)



**CHALMERS**  
UNIVERSITY OF TECHNOLOGY